

Synopsis of the thesis

**Characterization of 7075 Aluminium Alloy using Modifier
and Heat Treatment**

Submitted for the award of a degree

of

DOCTOR OF PHILOSOPHY

in

Metallurgical and Materials Engineering

by

Devangkumar Vishnuprasad Mahant

Department of Metallurgical and Materials Engineering,
Faculty of Technology and Engineering,
The M. S. University of Baroda,
Vadodara.

Guided by

Dr Vandana J. Rao

Department of Metallurgical and Materials Engineering,
Faculty of Technology and Engineering,
The M. S. University of Baroda,
Vadodara.



सत्यं शिवं सुन्दरम्

February 2023

Details of PhD Registration for Synopsis

1. Name of the faculty : Faculty of Technology and Engineering
2. Name of the PhD Scholar : Devangkumar Vishnuprasad Mahant
3. Registration No. : FOTE/872
4. Previous degree : ME (Industrial Metallurgy)
5. Area of research : Nonferrous Aluminium alloys (7075)
6. Title of the thesis : Characterization of 7075 Aluminium Alloy using Modifier and Heat Treatment
7. Research guide : Dr Vandana J. Rao
8. Department/Institution : Department of Metallurgical and Materials Engineering,
Faculty of Technology and Engineering,
The M. S. University of Baroda,
Vadodara- 390 001, Gujarat, India.
9. Date of Synopsis submission :

Table of Content

Details of PhD Registration for Synopsis	i
Table of Content.....	ii
List of Figures	iii
List of Tables	iv
1. Title of the thesis and abstract.....	1
2. Brief description of the state of the art of the research topic.....	4
2.1 7XXX aluminium alloys	5
2.2 Effect of grain refiners and modifiers on 7XXX aluminium alloys	5
2.3 Solidification of 7XXX aluminium alloys.....	8
2.4 Phase diagram of 7XXX aluminium alloy and heat treatment	11
3. Definition of the problem	13
4. Objective of the work	14
5. Original contribution by the thesis	14
6. Methodology of research and results & discussion	15
6.1 Phase I: Effect of the oxide addition into cast Al 7075.	15
6.2 Phase II: Effect of quenching medium on cast Al 7075.	20
6.3 Phase III: Effect of double-step ageing on the oxide-added cast Al 7075	22
6.4 Phase IV: Effect of different casting techniques on cast Al 7075	23
6.5 Phase V: Development of cast Al 7075 by alloy addition.....	25
7. Conclusions.....	26
8. List of publications:	29
9. References.....	31

List of Figures

Fig. 1 Casting process parameters, grain refiner/modifiers, and quenching media correlation to structure and segregation pattern.....	9
Fig. 2 Schematic presentation of constitutional supercooling and undercooling effect on the growth and grain morphology [94].....	10
Fig. 3 (a) Quaternary phase diagram of Al-Zn-Mg-Cu [103]; (b) binary phase diagram of Al-Zn for a temperature range of solution treatment and precipitation treatment [104]; (c) schematic presentation of ageing time v/s strength [105]; and (d) difference in the GP I and GP II [106].	11
Fig. 4 Methodology to produce oxide-added cast Al 7075.....	15
Fig. 5 Experimental setup and samples a) schematic of the experimental setup; b) dimensions of metallic die; c) tensile specimen dimensions as per ASTM E8M.....	16
Fig. 6 Optical microstructure of Al7075; a) as-cast; and 2.5 wt.% added b) ZrO ₂ ; c) TiO ₂ ; d) ZrTiO ₄ ..	17
Fig. 7 Graphical presentation of mechanical properties of Al 7075; as-cast, and 2.5 wt.% added oxides.	18
Fig. 8 SEM photographs of; (a) as-cast Al7075; (b to f) ZrO ₂ -added Al7075; (g) TiO ₂ -added Al7075; (h) ZrTiO ₄ added Al7075.	18
Fig. 9 Schematic diagram of quenching of cast Al 7075 during solidification in; a) ice, b) hot water for 30 min, and c) hot water until cooled down.....	20
Fig. 10 Micrographs of cast Al 7075; a) as-cast, b) ice quench, c) hot water for 30 min, and d) hot water until cooled down; Micrographs of cast Al 7075 (naturally aged for 2 years) e) as-cast, f) ice quench, g) hot water for 30 min, and h) hot water until cooled down.....	20
Fig. 11 Elemental mapped EDS layered images of Al 7075; a) as-cast, b) ice, c) H30, and d) HTC.....	22
Fig. 12 Double-step ageing cycle for oxide-added cast Al 7075	22
Fig. 13 Optical micrographs of oxide-added cast Al 7075 of as-cast, ZrO ₂ -added, TiO ₂ -added, and ZrTiO ₄ -added before heat treatment (a-d) and after heat treatment (e-h), respectively.....	23
Fig. 14 Schematic illustration of casting techniques; a) gravity die casting, b) sand casting and c) investment casting.	24
Fig. 15 Optical micrographs of different casting techniques of cast Al 7075; a) gravity die casting, b) sand casting, and c) investment casting; naturally aged (d-f), respectively.	24
Fig. 16 Methodology of developed cast Al 7075.....	25
Fig. 17 Optical micrographs of Al 7075; a) developed cast 7075, b) cast 7075 from wrought, and c) wrought 7075.....	26

List of Tables

Table 1 chemical composition of 7075 aluminium alloy as per standard [26]–[28].	5
Table 2 Details elements or reinforcement, additives, grain refiners addition, methodology, and properties reported by researchers.	5
Table 3 Environment-sensitive embedding energy of Zn, Mg, and Cu at the grain boundary and α -Al [101].	10
Table 4 Spectroscopy of the as-received 7075-T6 aluminium alloy.	16
Table 5 Physical properties and Chemical analysis of high-temperature oxides.	16
Table 6 Chemical analysis of Al7075 alloy in; A) as-cast conditioned, B) 2.5 wt.% ZrO ₂ , C) 2.5 wt.% TiO ₂ , D) 2.5 wt.% ZrTiO ₄ .	17
Table 7 EDS analysis of Zr and Ti amount in the oxide-added cast Al 7075.	17
Table 8 EDS analysis of selected point/area in Fig. 8 (in wt. %) and closest intermediate phases.	19
Table 9 Mechanical properties of Al 7075; as-cast, quenched in ice, hot water for 30 min (H30), and hot water until cooled down (HTC).	21
Table 10 Mechanical properties of as-cast, ZrO ₂ -added, TiO ₂ -added, and ZrTiO ₄ -added cast Al 7075 before and after heat treatment.	23
Table 11 Mechanical properties of cast Al 7075 by different casting techniques.	25
Table 12 Comparative Mechanical properties of cast and wrought 7075 alloys.	26

1. Title of the thesis and abstract

Title of the Thesis: Characterization of 7075 Aluminium Alloy using Modifier and Heat Treatment.

Abstract:

Wrought 7075 aluminium alloy is a prevalent high-strength and lightweight in the automobile and aerospace industries. The 7075 quaternary alloy having primary alloying elements is Zn; others are Mg and Cu. There is a broad applicability of Al7075 in wrought conditions after machining, which is costlier and time-consuming. The casting route is cost-effective but has a problem with hot tearing and solute segregation due to its wide solidification range. The solidification behaviour of 7XXX aluminium alloy is a little sluggish due to its three elements and distribution within the α -Al matrix.

There are ways to alter the segregation pattern during solidification and finally into the microstructure. The same can be possible thermally, chemically and mechanically or by combining any two treatments. This research mainly focuses on modifying the solute position within the microstructure by creating heterogeneous nucleation sites. The high-temperature oxides like ZrO_2 , TiO_2 , and $ZrTiO_4$ create heterogeneous nucleation sites and alter the solidification behaviour after casting. The results are compared with those without oxide-added cast Al 7075. The oxide powders were added with a fixed 2.5 weight percentage. SEM was carried out to check the oxide particle size, and EDS was done to check the chemical composition of the as-received powders and their purity. The final oxide-added samples of Al7075 were studied in detail using microstructure examination, SEM-EDS study to check the local chemistry, and XRD analysis to confirm the generated phase. Among all the oxides addition, the best mechanical properties and microstructure modification were observed in 2.5 wt.% ZrO_2 -added Al 7075. The higher mechanical properties were achieved due to the reduction in average grain diameter and uniform distribution of the intermediate phases like $\eta(MgZn_2)$, $S(Al_2CuMg)$, and $T(AlCuMgZn)$ in the α -Al matrix. SEM-EDS and XRD confirmed the presence of the intermediate phases. SEM-EDS analysis was also used with a different approach to determine the closest intermediate phase by checking an elemental ratio of Zn/Mg in the micrograph. Further, all the micro

samples were kept for two-year to understand the effect of natural ageing. The change in the intermediate phase distribution was observed, and microhardness was recorded.

To understand the segregation issue caused by solid-liquid interface movement and solute rejection by the solid phase during solidification, the effect of controlled diffusion solidification by quenching cast Al7075 was also investigated. The cast Al7075 was quenched in three variants: ice water, hot water for 30 minutes and hot water until it cooled down. The mould was kept in the ice and hot water while pouring the melt. The effect of quenching was observed on microstructure and mechanical properties both. The non-equilibrium intermediate phase distribution was observed within the α -Al matrix. The effect of ice and hot water influenced the formation of primary α -Al and eutectic phases. The observed eutectic phase morphology differed from dendritic to non-dendritic for ice-quenched Al 7075. The best results were achieved for 30 min quenching in hot water, i.e. 197 MPa UTS and 100 BHN.

The solutionizing heat treatment attributes temperature-dependent equilibrium solid solubility of 7XXX aluminium alloys, and quenching in water provides a supersaturated solid solution which produces solute clusters. The time-dependent low-temperature ageing treatment below equilibrium solvus temperature forms translational precipitates. The third phase of the present research work includes the effect of heat treatment response for high-temperature oxides added cast Al 7075. The oxides like ZrO₂, TiO₂, and ZrTiO₄ were added to cast Al 7075 and heat treated by solution treatment followed by double-step ageing. Usually, Al 7075 is age-hardened by T6 treatment (artificially aged), but in the present study, double-step ageing was given to oxide-added cast Al7075. The samples were solutionized at 480 °C for 1hr for homogenization and then quenched in cold water to get a supersaturated solid solution (α_{SSSS}) followed by double-step ageing at 100 °C for 4 hr + 135 °C for 17 hr. The microstructure, mechanical properties, SEM-EDS, and XRD analysis were performed to study the effect of double-step ageing of oxide-added Al 7075. The highest mechanical properties were achieved in the ZrO₂-added Al 7075 before and after double-step ageing. The homogeneous distribution of precipitates improved the mechanical properties. The tribology study was also performed on the samples before and after heat treatment. The wear rate of ZrO₂-added Al 7075 is low, and a

comparison of the wear mechanism was also studied for the as-cast and other oxide-added samples.

The different casting techniques have advantages and disadvantages by considering the mechanical properties and applications due to the changes in the solidification pattern of the cast alloys. The heat dissipation from a different mould generates the thermal gradient and controls the microstructure and mechanical properties. Three casting methods, permanent mould casting (gravity die casting), green sand casting, and investment casting, were used to check the solidification pattern. The microstructure, mechanical properties, and SEM-EDS analysis were performed to understand the segregation pattern and response of the different casting techniques. The tensile strength achieved by gravity die casting is 183 MPa. The hardness value after gravity die casting is 59 BHN, 100 BHN in green sand casting, and 86 BHN in the case of investment casting. The observed high hardness is due to the formation of eutectics within the grain and interdendritic channels at grain boundaries.

Wrought Al 7075 is very costly in the market. From the market survey, the cost per kilogram varies between Rs. 600 to 950 and is even higher. Attempts were made to develop 7075 alloys by adding alloying elements into the pure aluminium in a resistance heating furnace to reduce cost. The four attempts were performed, and the last attempt successfully adjusted the final chemistry of Al 7075 as per the standard. The addition of the alloying elements and their sequence is a crucial parameter while developing an alloy. The design of an alloy was adjusted by considering the recovery of alloying elements. The final chemical difference was adjusted in the next heat. The microstructure and mechanical properties were compared with wrought Al 7075. The developed alloy costs Rs. 280 to 300 per kg, 50% lower than the market price.

The insightful research on the characterization of Al 7075 was done by using modifiers and heat treatment to change the segregation pattern and microstructure, and finally, the mechanical properties. The effect of quenching and different casting techniques are also studied in detail.

2. Brief description of the state of the art of the research topic

Wrought Al 7075 alloy is well-known in the area of aerospace industry and automobile sectors. Such materials reduce the problem of CO₂ emission due to high-strength and low-weight ratios. The cast properties of nonferrous alloys do not match with wrought properties of the same. Cast products have problems with porosities, segregation, and grain size, which reduces the mechanical properties. Solute segregation is the main problem of cast 7075 aluminium alloy.

Many techniques are studied to improve the cast properties of 7075 alloys. It is categorized into three major areas; the addition of oxides, modification of the heat treatment cycle, and the micro-alloying effect [1], [2]. Many researchers studied the addition of oxides, carbides, and nitrides in aluminium alloys to improve the structure-property relationship. The addition of Al₂O₃, TiO₂, TiC, SiC, AlN, and numerous other additives is investigated in Al alloys, including Al7075 [3]–[8]. The other technique includes a heat treatment cycle named the diffusion-controlled solidification process can alter microstructure [9], [10]. The micro-alloying effect includes grain refinement of cast alloy by adding a small quantity of Zr, Sc, Sr, Ag, Er, Ti-B₂, and other rare earth metals [11]–[16]. The 7XXX aluminium alloy has Zn, Mg, Cu, and Cr solutes. The solute redistribution during solidification leads to micro-segregation and the formation of coarse intermetallic particles, which can significantly influence the properties of the 7000 series aluminium alloys [17]. With decreasing Zn/Mg ratio, the density of MgZn₂ phases in the grain interior increased, and precipitates were observed at the grain boundary. The strength of these alloys generally depends on Zn to Mg ratio [18]. It has the problem of hot cracking during rapid cooling even with a Zn concentration of around 7 to 8 wt.% [19]. The as-cast microstructure involves α (Al), eutectic of (α (Al) + Mg (AlCuZn)₂), and Al₇Cu₂Fe phases [20]. The small addition of zirconium can improve its properties by forming metastable and coherent Al₃Zr dispersoids, which prevent recrystallization through a grain boundary pinning mechanism [21].

2.1 7XXX aluminium alloys

7XXX aluminium has zinc as the primary alloying element, in amounts of 1 to 8 wt. %. The small amount of magnesium improves strength by making it heat-treatable. Other elements, copper and chromium, are added in smaller quantities [22]. The chemical composition of 7075 aluminium alloy as per the standard is presented in Table 1. As a principal alloying element of zinc, the commercial Al-Zn-Mg alloy forms phases by eutectic decomposition: hcp $MgZn_2$ and bcc $Al_2Mg_3Zn_3$ during solidification. These two metastable phases strengthen this copper-free alloy, and the formation depends on the zinc/magnesium ratio. The copper-containing Al-Zn-Mg-Cu alloy, where copper and aluminium substitute zinc in $MgZn_2$ and formed $Mg(Zn,Cu,Al)_2$, and Al_2CuMg by eutectic decomposition or solid-state precipitation [22]–[25].

Table 1 chemical composition of 7075 aluminium alloy as per standard [26]–[28].

Alloy	Wt.%						
	Zn	Mg	Cu	Mn	Cr	Si (max)	Fe (max)
7075	5.1 – 6.1	2.1-2.9	1.2-2.0	0.30	0.18-0.28	0.40	0.50

2.2 Effect of grain refiners and modifiers on 7XXX aluminium alloys

Many researchers added oxides [29]–[37], carbides [29], [30], [46]–[54], [38]–[45], nitrides [55]–[60], borides [61]–[64], and other micro-alloying elements in Al 7075. The summary of the wide literature survey is presented in Table 2.

Table 2 Details elements or reinforcement, additives, grain refiners addition, methodology, and properties reported by researchers.

Elements/Reinforcement/Additive/Grain Refiners	Methodology	Properties	Discussion	Ref
Al-4.5Cu-0.3Mg-0.05Ti+ Zr (0.05wt. %-0.5wt. %)	Die Casting Route (Master alloys Al-5Ti-1B + Al + Mg+ Cu-50Al) remelted for Zr addition	UTS (217-250 MPa)	Coarse Al_3Zr particles are present in the intergranular regions.	[65]
Al7075+Al-2Sc and Al-15Zr	Die Casting Route + thermo-mechanical treatment	Peak Hardness 195 BHN with 50% Rolling at 100 °C + UTS 611 MPa Peak Hardness 160 BHN with 30% Rolling at 100 °C + UTS 612 MPa	$Al_3(Sc, Zr)$ nano-dispersoids are uniformly distributed throughout the microstructure.	[66]

Al-Zn-Mg-Cu-Sc-Zr+ Er content (0-0.4%)	Die casting Route	0.4% Er - corrosion potential was reduced due to Al ₈ Cu ₄ Er and Al ₃ Er, two phases that enhanced the potential difference between the grain boundary and the matrix.	Er controls the microstructure; the dendrite arms and grains size are refined first, then coarsened and refined again.	[67]
7075-T6+Reinforcement by SiC	vortex casting method + nano, submicron and micron SiC added	Nano (1wt.%) - 682 MPa Sub-micron(2wt.%) - 652 MPa Micron(2wt.%) - 627 MPa	For micron particles, the final tensile strength was improved in specimens with 2 wt. %.	[68]
7075 alloy powder with 1 wt.% Ti submicron particles (0.2 - 2 μm)	Selective laser melting (SLM)	UTS - 291 ± 19 MPa; EL- 7.9 ± 2.9%. After T6 - UTS 503; ± 6 MPa; EL - 7.5 ± 1.2%	Inoculation of 7075 by Ti powder produced crack-free, fine-equiaxed microstructure.	[69]
Al7075+Nb	Ingot Casting + Melt spinning	The micro-hardness of 0.5 wt.% Nb- 0.9 GPa. 3 times more than without added Nb.	Nb addition modified the dimensions and shapes of both α-Al and intermetallic phases. The average grain size reduced from 9.1 μm to 2.46 μm.	[70]
Al7075+ (WC-Co) (50 μm)	Addition of Cermet 3, 6, and 9 wt. % by Stir Casting	UTS 193 MPa; EL-1.86 for 9 wt.% 108 BHN	Increases the yield stress and tensile strength by 49% and 58% but drastically decreases the percentage elongation by 84%.	[71]
Al7075+6wt.%SiC (~20 μm)	Stir Casting	Wear of 10N, 2 m/s sliding speed, 500 m sliding distance - optimum wear	Wear mechanism by SEM, abrasive wear and ploughing.	[72]
Al7075+Si ₃ N ₄ (2 to 8) wt.% increase 3%, HfC (0.5 to 2) wt.% increase 0.75% and MoS ₂ (2 to 5) wt.% increase 1.5 %	Stir Casting	UTS- 209 MPa, EL-24.2 Hardness - 152 VHN, Fatigue stress - @70Kg; 17653 cycles - No failure	Al7075+5wt.% Si ₃ N ₄ +1.25wt.% HfC+3.5wt.% MoS ₂ shows the optimum result of tensile and fatigue due to the fine grain size.	[73]
Al7075+0.2 Graphene	Die-Cast	refined the grain size of 7075 Al alloys from 78 μm to 45 μm	Graphene can promote heterogeneous nucleation and has little effect on the thermal properties of as-cast 7075.	[74]

Al7075+(0-20 Vol.% SiO ₂) +Foaming agent	Direct Melt Foaming Method	the grain size of α -Al is reduced, forming MgAl ₂ O ₄ , MgO, Al ₂ O ₃ , and Mg ₂ Si	The refining effect of the SiO ₂ is due to heterogeneous nucleation of the α -Al grain by SiO ₂ particles or restriction of the α -Al grain growth.	[75]
7075+TiB ₂ (3-6 wt. %)	Rheocasting	Before HT - 70BHN After HT - 75BHN Rheocast has a lower Wear rate than die-cast.	The average grain sizes are 23 μ m, and the shape factors are 0.96 of rheocast 4.5 wt.% TiB ₂ /7075	[76]
Al7075+Nano TiO ₂ (5 and 10wt. %)	Stir Casting	As cast -70 BHN; UTS-212 MPa 5wt.% TiO ₂ -78 BHN; UTS-247 MPa 10 wt.% TiO ₂ -99 BHN; UTS-298 MPa	The volumetric wear loss of matrix and TiO ₂ particles reinforced nanocomposites increased with increasing applied load and speed.	[77]
Al7075+ (0.1 - 0.6 wt. %) Sc (Micro-alloying)	Die-Cast + addition by master alloy +Hot rolling + Solution treatment followed by ageing treatment	1. 0.6 wt.% Sc -128 HV; 2. After homogenization@ 460°C for 10h -Micro-hardness - 98 HV; UTS - 195 MPa; 3. Via hot rolling@400 °C;50% reduction, solution (470°C for 1h and aging treatment 120°C for 24h) - 152HV, UTS - 450 MPa	Sc significantly reduces the grain size from 129.92 μ m to 32.17 μ m with 0.6% Sc	[78]
Al7075+ (1-4 wt. %) TiB ₂	AM (Laser Melting deposition)	Optimum properties of 4wt. % TiB ₂ 127.8 HV	The grain size decreased by 32 % compared with the unreinforced 7075 Al specimen.	[79]
Al7075+5wt.% nano B ₄ C + 10 wt.% of Al ₂ O ₃ and improved by 2,4,6 and 8wt.% of ZrO ₂ nanoparticles"	Stir Casting	Al7075 HMMCS + 8wt. % ZrO ₂ has less wear resistance.	The wear resistance increased as the weight fraction of ZrO ₂ increased within Al 7075 hybrid nanocomposite.	[80]
Al7075 + (0.5,1.5 & 2.5 wt. % ZrO ₂) (50-75 μ m)	Stir Casting	2.5 wt.% ZrO ₂ Hardness - 122 HV UTS - 131 MPa; EL - 4.7%	The hardness, strength of yield, and tensile strength increased with increasing the weight % of ZrO ₂ to 2.5 wt. % while the elongation decreased.	[81]
Al7075+ (3, 6, 9, 12 wt. %) (5-11 μ m)	Compocasting process	6 wt. % ZrO ₂ Hardness -61.3 BHN UTS - 148 MPa	A large increase in the properties was observed up to 6	[82]

			wt.%, and the improvement is minimal after that.	
Al 7075+X wt.% B ₄ C+2wt.% Fly-ash (X= 2,4,6,8)	Stir Casting	(Al 7075/2 wt.% FA/8 wt.% B ₄ C) micro-hardness - 123.29 HV, 37.2% higher than base matrix alloy	Adding B ₄ C and fly ash increases the micro-hardness of the casted composite.	[83]
AA7075+1 vol % TiC (molten salt-assisted processing NP)	Stir Casting	Nan-treated TiC AA7075 - 188 HV As-cast AA7075 - T6 - 165 HV	After T6 treatment, an average grain size of 18.5 μm.	[6]

The literature summary indicates the important changes in the mechanical properties by the addition of oxides, carbides, borides, and nitrides into 7075 alloys. Imran et al. [39] have conducted a detailed survey on the mechanical properties of aluminium matrix composites. After grain refinement, micro-sized and nanosized particles improved tensile strength range between 132 - 312 MPa and 400 - 590 MPa, respectively, while as-cast tensile strength was achieved from 88 - 275 MPa [84]-[93]. The comparative study of ZrO₂, TiO₂, and ZrTiO₄ oxide-added cast Al 7075 remains unexplored, and natural ageing behaviour is also novel. Most of the studies focused on the mechanical and tribological properties, but very few focused on the segregation pattern and Zn/Mg ratio to determine the closest intermediate phase's presence.

2.3 Solidification of 7XXX aluminium alloys

Solidification begins with the appearance of nuclei, and when the cluster of atoms come together during random motion in the melt, termed embryonic crystals, that permit further sitting of atoms on their surfaces, which causes the solid phase growth [94]. It is well known that nucleation and growth are fundamental to understanding the solidification of alloys. The solidification of alloys is solidified over a range depending on alloying elements, thermal gradient, and degree of undercooling. The addition of (cold) oxides (foreign particles), impurities, or even the mould wall provides a heterogeneous nucleation site that controls the final microstructure. It is known that heterogeneous nucleation requires less activation energy than homogeneous nucleation. Solidification of cast Al 7075 studies can contribute to understanding emerging processing like selective laser melting, additive manufacturing, 3D printing technology and many more [95]-[97].

Segregation of solutes during solidification refers to the non-uniformity of the chemical composition. The patterns of solute distribution result in a segregation pattern that may be considered a chemical structure. Morphology development and segregation pattern are intertwined phenomena and can be subdivided into macro-segregation and micro-segregation. Micro-segregation is complex in the multicomponent system. Earlier refinement treatment and dendrite tip undercooling treatment were employed. Macro-segregation results from localised micro-segregation due to the physical movement of the liquid and solid phases [98]. Also, non-equilibrium solidification is accompanied by a certain degree of micro-segregation due to partitioning between a solid-liquid interface [99]. The development of morphology by process parameters was studied in the literature. Fig. 1 shows the correlation of the casting process, grain refiners and modifiers, and quenching media influence on the microstructure and segregation pattern.

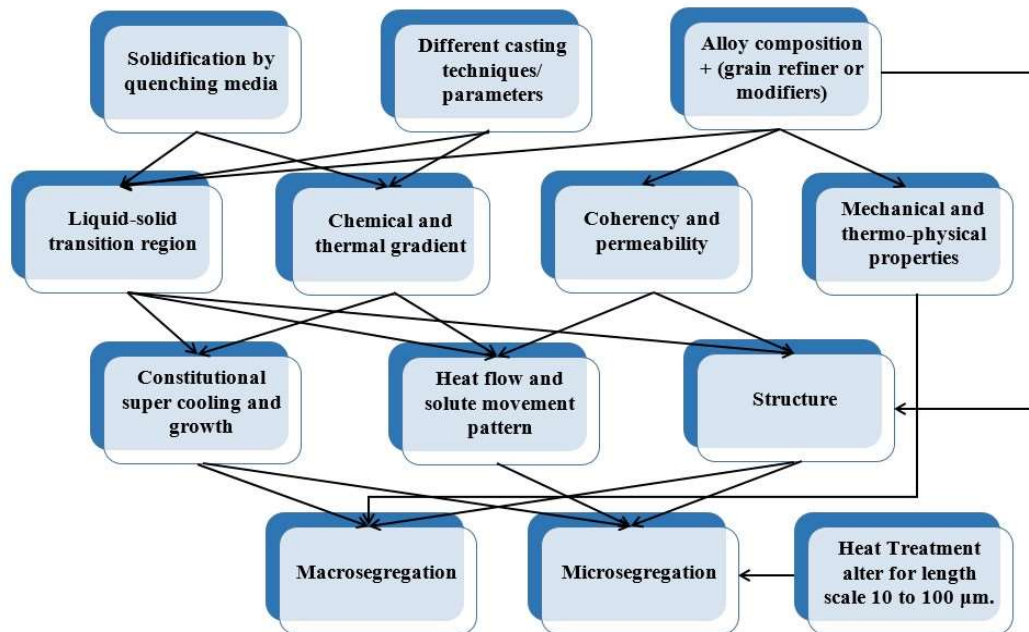


Fig. 1 Casting process parameters, grain refiner/modifiers, and quenching media correlation to structure and segregation pattern

During solidification, solutes are mainly distributed within the grain, segregate at grain boundaries, and freeze in the interdendritic region depending on the solidification behaviour. Xiao et al. [100] studied models for predicting critical interface velocity and found that the presence of nanoparticles produces a difference in growth velocity at the S/L interface. Also, the formation of cellular interface

inspired by splitting interface due to the constitutional supercooling of surrounding melt and segregation of solutes behind the particles. Fig. 2 indicates the effect of constitutional supercooling and undercooling on grain growth and morphology.

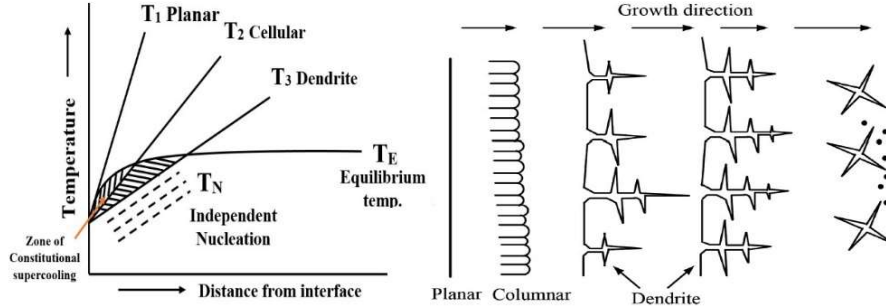


Fig. 2 Schematic presentation of constitutional supercooling and undercooling effect on the growth and grain morphology [94].

For the segregation of solute elements, Liu et al. environment-sensitive embedding energy from Eq. 1 found that for a large value of environment-sensitive embedding energy, more solute atoms are influenced by the environment around it, becoming unstable and diffusing to the stable environment where this energy is low [101].

$$E_{ESE} = [E_i - (n - 1) E_{self} - E_{iself}] - (E_{cl} - nE_{self}) \dots \dots (1)$$

E_i is the structural energy with a solute atom, E_{cl} is the structural energy without a solute atom, n denotes atomicity, E_{self} is the matrix atomic energy, and E_{iself} is the matrix-solute atomicity energy. The calculated environment-sensitive embedding energies for Zn, Mg, and Cu are indicated in Table 3.

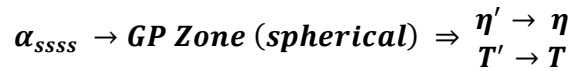
Table 3 Environment-sensitive embedding energy of Zn, Mg, and Cu at the grain boundary and α -Al [101].

Position	Zn	Mg	Cu
At grain boundary	1.6452	21.9444	22.6892
In α -Al	1.1292	22.5959	23.0077

From the above table, the ESE of Zn in the α -Al grain matrix is lower than the grain boundary, so Zn atoms are distributed uniformly within the matrix. While ESE of Mg and Cu is higher than Zn atoms within the α -Al matrix, so lower solid solubility. Hence Mg and Cu atoms are found at grain boundaries. Moreover, Cu has the highest ESE in the α -Al matrix, so solid solubility is to be the least [7].

2.4 Phase diagram of 7XXX aluminium alloy and heat treatment

The heat treatment for 7XXX alloys is to get uniform distribution of Zn, Mg, and Cu atoms in the Al matrix, which increases homogeneous solute atom clustering. It is a well-known precipitation transformation sequence, as below.



As discussed in section 2.3, a wide solidification temperature range develops heterogeneous microstructure, and the secondary phases form at the interdendritic channel and the grain boundary [102].

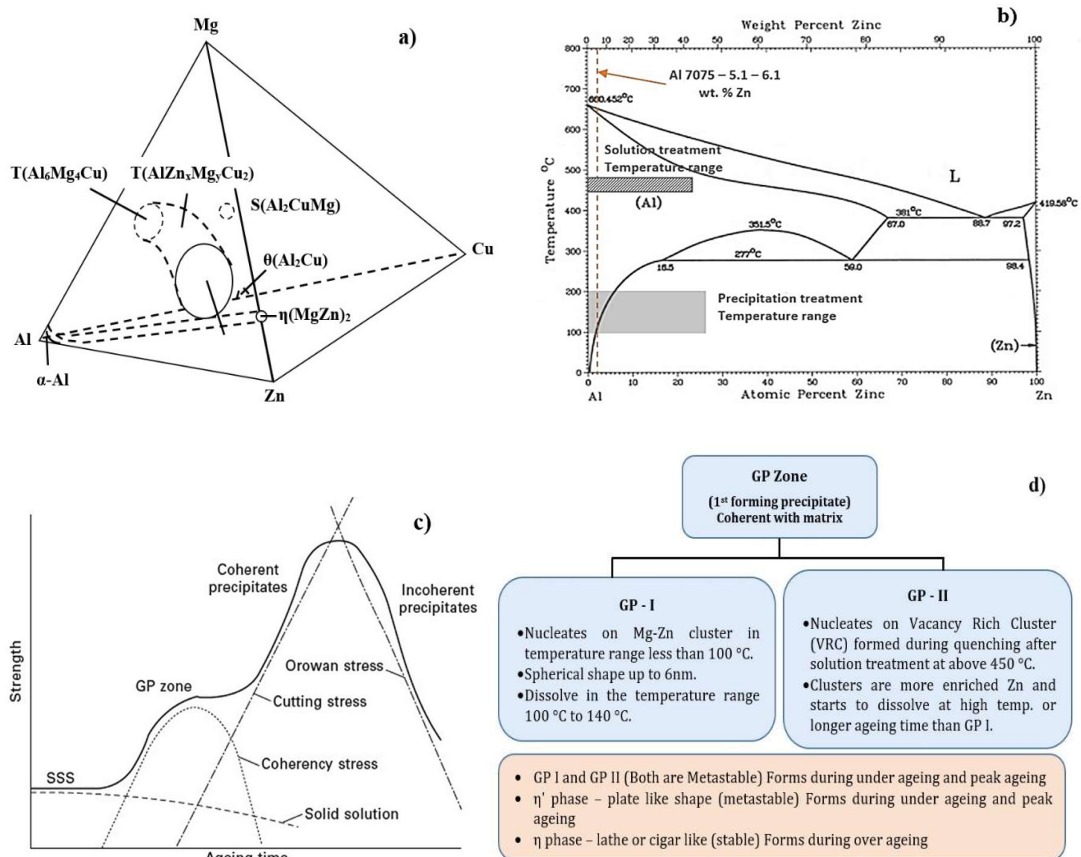


Fig. 3 (a) Quaternary phase diagram of Al-Zn-Mg-Cu [103]; (b) binary phase diagram of Al-Zn for a temperature range of solution treatment and precipitation treatment [104]; (c) schematic presentation of ageing time v/s strength [105]; and (d) difference in the GP I and GP II [106].

The phase diagram for the Al 7075 quaternary alloy is shown in Fig. 3(a). The binary diagram of Al-Zn is presented to understand the solution and precipitation treatment temperature zone in Fig. 3(b). The effect of ageing on the formation of precipitation

sequence with strength and difference in GP I and GP II is shown in Fig. 3(c) and Fig. 3(d), respectively. Fig. 3(a) shows the presence of the intermediate phase according to four component phase behaviour in a pyramid-shaped diagram (tetrahedron). Many researchers studied the formation of eutectic phases like η , T ($\text{Al}_2\text{Mg}_3\text{Zn}_3$), S, θ , ($\text{Al}_7\text{Cu}_2\text{Fe}$) in Al 7075 and their segregation during casting [13], [95], [107]. The increasing Mg content increases strength and hardness but lowers the elongation and also enlarges the area fraction of the grain boundary intermediate phases [108]. Shu et al. [109] showed that the microstructure of Al-Zn-Mg-Cu alloys contains intermetallic phases like $\theta(\text{Al}_2\text{Cu})$, $\text{Mg}(\text{Zn}, \text{Al}, \text{Cu})_2$, along with $\alpha(\text{Al})$ during the microstructural evolution process, the evolution process follows patterns like $\text{Liq.} \rightarrow \text{Liq.} + \alpha(\text{Al}) \rightarrow \text{Liq.} + \alpha(\text{Al}) + \sigma[\text{Mg}(\text{Zn}, \text{Cu}, \text{Al})_2] \rightarrow \text{Liq.} + \alpha(\text{Al}) + \sigma[\text{Mg}(\text{Zn}, \text{Cu}, \text{Al})_2] + \theta(\text{Al}_2\text{Cu})$ and validated that the solidification paths as per the Scheil model.

The 2XXX, 6XXX and 7XXX aluminium alloys are hardened by precipitation hardening. The as-cast structure formed the coarse eutectic phases at the grain boundary. Precipitation is the solid-state transformation which requires a driving force like surface and strain energy. In solution treatment, the alloy is heated above solvus temperature until a homogeneous solid solution forms and is rapidly quenched to get a supersaturated solid solution within the α -Al matrix. Then, an alloy is heated below the solvus line to diffuse it on nucleation sites and form the finely dispersed precipitate. The strengthening of the alloy depends on the formation of the types of soft and hard precipitates. Coherent precipitates are formed by under and peak ageing, while incoherent precipitates are formed by over-ageing [110].

Fig. 3(c) shows that at the peak ageing (T6) treatment, the higher strength is due to the formation of η' precipitation. M. Khan et al. [23] found that variation in the formation of grain boundary precipitates mainly exists θ'' precipitates with few η' precipitates at low-angle grain boundary during peak ageing while in double-ageing found at the high-angle grain boundary. Very few literature surveys are available on double-step or duplex ageing of Al 7075. Zhang et al. [111] studied double-step ageing treatment of Al-5Mg-3Zn-1Cu at 120 °C for 1 hr and at 150 °C for 4 hr from 156 to 5 hr peak ageing and achieved comparative properties. Siddesh et al. [112] prepared a critical survey on heat-treatable aluminium alloys, but natural and double-step ageing are not summarized due to less available research.

3. Definition of the problem

The major challenge is the application of Al 7075 by the casting route due to the solute segregation problem. The production of Al7075 by casting route can potentially replace the costlier processing of wrought 7075 aluminium alloy. As per the literature survey, the wrought 7075 aluminium alloy has high strength, nearly similar to steel. The forming processes and secondary operations to get the final product is significantly costlier. Many researchers studied cast Al 7075 by adding grain refiners, modifiers, and microalloying elements to achieve significant mechanical properties. After an extensive literature survey, the present study focuses on changing the eutectic phase segregation pattern by adding high-temperature oxides like ZrO_2 , TiO_2 , and $ZrTiO_4$ in the cast Al7075 by die casting route. The comparative effect of these three oxides on the cast Al 7075 and their natural ageing is a novel study. However, the study on the solute segregation pattern and the intermediate phase formation within the microstructure is quite complex but essential to solving the problem of cast Al 7075.

A detailed discussion in the literature, the addition of grain refiners or modifiers (chemically), controlled diffusion solidification (thermally), mould vibration (mechanically), or a combination of either can alter solute segregation patterns. Another aspect of the study is focused on microstructural morphology and mechanical properties by quenching cast Al7075 in ice, hot water for 30 minutes, and hot water until cooled down. A similar work is hardly reported in the present literature. Further, a study on the different casting techniques is performed to produce the cast Al 7075 by permanent mould casting (gravity die casting), sand casting, and investment casting. The mould characteristics play a significant role in the solidification of cast Al 7075, which influences the solute segregation and phase morphology of the final microstructure.

The double step-ageing of oxide-added cast Al 7075 is studied to compare microstructure and mechanical properties before and after the heat treatment. SEM-EDS and XRD analysed the precipitate phase to understand the precipitation behaviour. The double-step ageing cycle is unique, as most literature studied

conventional T6 treatment, retrogression and re-ageing or either homogenization treatment.

The cast Al 7075 was developed by alloying and compared the microstructure and properties with the wrought Al 7075. The motivation for development is the high cost of the wrought Al 7075. The chemistry was achieved after the four successive heats, but achieving mechanical properties is challenging. However, the developed as-cast results are promising compared to as-cast Al 7075 produced from Al 7075-T6.

4. Objective of the work

The following objectives based on the research gap are discussed below:

1. To study the effect of the addition of high-temperature oxides in the cast Al 7075 to understand the segregation pattern.
2. To study the effect of quenching media on cast Al 7075 to understand the eutectic phase morphology change.
3. To study the effect of double-step ageing treatment on oxide-added Al 7075 to understand the effect of modified heat treatment on microstructure, mechanical, and tribology properties.
4. To study the microstructure and mechanical properties of cast Al 7075 by different casting techniques.
5. To develop cost-effective cast Al 7075 by alloy addition and compare its properties with wrought Al 7075.

5. Original contribution by the thesis

The thesis's original contribution is studied on the subjective research gap of Al 7075.

The followings are significant contributions:

- 1) Development of ZrO_2 , TiO_2 , and $ZrTiO_4$ oxide-added cast Al 7075.
- 2) Investigation of segregation pattern and phase morphology and their effect on mechanical properties.
- 3) Study on the effect of quenching media during casting of Al 7075.
- 4) Study on the effect of double-step ageing on oxide-added cast Al 7075.
- 5) Comparison of the microstructure, mechanical, and tribology properties of cast Al 7075 after double-step ageing (before and after).

- 6) Study the changes in the different casting techniques to alter the segregation pattern of the eutectic phase.
- 7) Development of cost-effective cast Al 7075 by alloying additions.

6. Methodology of research and results & discussion

The present research is divided into five phases.

- Phase I** Effect of the oxide addition into cast Al 7075.
- Phase II** Effect of quenching medium on cast Al 7075.
- Phase III** Effect of double-step ageing on the oxide-added cast Al 7075.
- Phase IV** Effect of different casting techniques of cast Al 7075.
- Phase V** Development of cast Al 7075 by alloy addition.

6.1 Phase I: Effect of the oxide addition into cast Al 7075.

The high-temperature oxides are added to the cast Al 7075 with the fixed 2.5 weight percentage. The separate addition of oxides like ZrO_2 , TiO_2 , and $ZrTiO_4$ act as a modifier in the melt of Al 7075. It provides a heterogeneous nucleation site to form nuclei. The comparative effect of oxide-added and as-cast microstructure and mechanical properties is studied based on the formation of a segregation pattern of solute within the α -Al matrix. The methodology is described in the flow diagram Fig. 4:

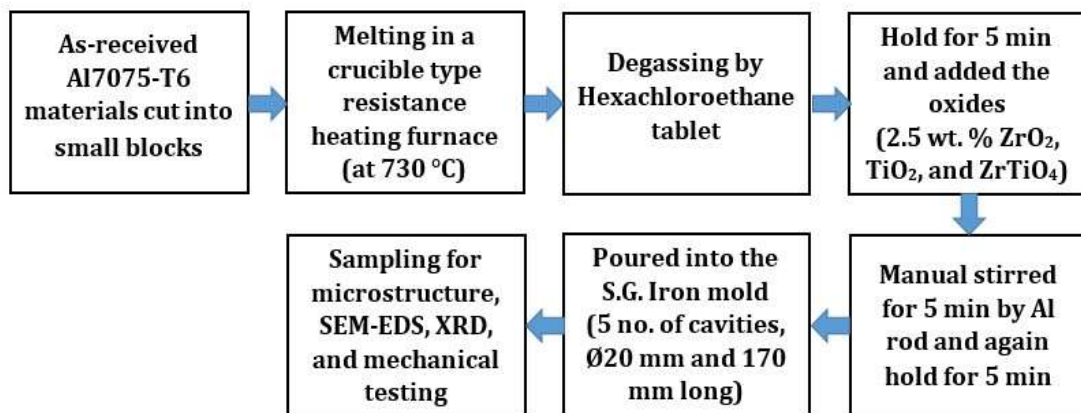


Fig. 4 Methodology to produce oxide-added cast Al 7075

The received materials were checked for chemical analysis by optical emission spectroscopy. The Thermo Fisher Scientific model ARL™ iSpark 8860 Fire Assay machine was used to perform chemical analysis.

Table 4 Spectroscopy of the as-received 7075-T6 aluminium alloy.

Element (wt. %)	Zn	Mg	Cu	Mn	Al
Average	5.48	2.25	1.54	0.09	90.64

The schematic diagram of the experimental setup and metallic die is shown in Fig. 5(a) and (b). The dimension of a tensile specimen is shown in Fig. 5(c) as per ASTM E8M. The physical and chemical properties of high-temperature oxides are given in Table 5. The chemical analysis of oxide-added and as-cast Al 7075 is presented in Table 6.

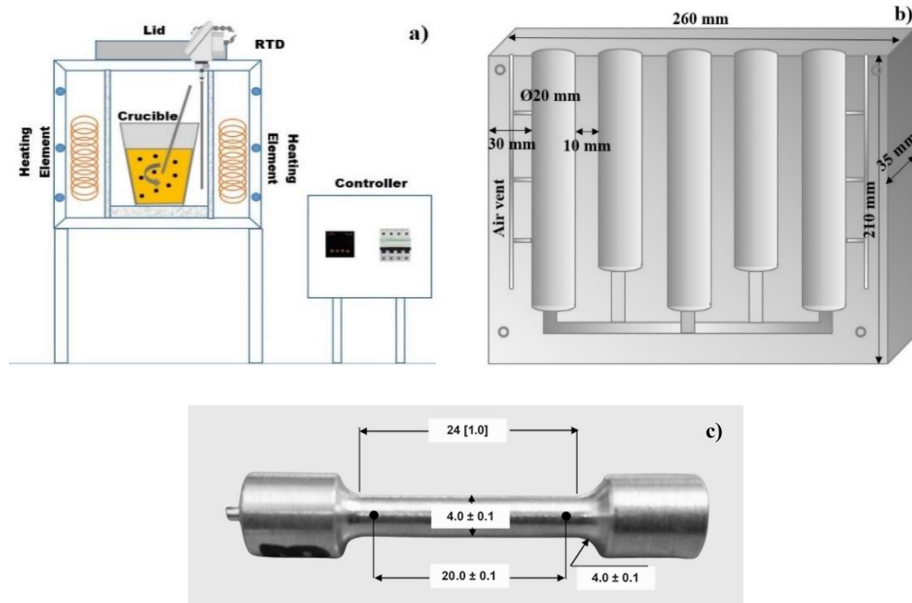


Fig. 5 Experimental setup and samples a) schematic of the experimental setup; b) dimensions of metallic die; c) tensile specimen dimensions as per ASTM E8M.

Table 5 Physical properties and Chemical analysis of high-temperature oxides.

High-temperature oxides (Powder Form)	Density (g/cc)	Crystal Structure	Chemical Analysis by SEM/EDS (wt.%)			Particle Size Measurement by SEM
			Zr	Ti	O	
Zirconium Oxide (ZrO_2)	5.68	Monoclinic	64.61	--	35.39	2-6 microns
Titanium Oxide (TiO_2)*	4.23	Tetragonal	--	29.80	57.36	
Zirconium Titanate ($ZrTiO_4$)	4.82	Orthorhombic	25.20	25.10	49.70	

*impurities such as Ca & Si in 3.42 & 9.24 wt. % respectively.

SEM-EDS analysis of Zr and Ti amount in the oxide-added cast Al 7075 is presented in [Table 7](#). The measured particle size of received oxides by SEM ranges between 2 – 6 microns.

Table 6 Chemical analysis of Al7075 alloy in; A) as-cast conditioned, B) 2.5 wt.% ZrO₂, C) 2.5 wt.% TiO₂, D) 2.5 wt.% ZrTiO₄.

Systems cast Al 7075	Elements (wt.%)					
	Zn	Mg	Cu	Cr	Zr	Ti
As-cast (A)	5.7223	2.4270	1.8060	0.2050	0.0001	0.0003
ZrO ₂ (B)	5.9810	2.2360	1.6180	0.2120	0.0118	0.0240
TiO ₂ (C)	5.8821	2.2290	1.5490	0.2040	0.0103	0.0280
ZrTiO ₄ (D)	6.0630	2.2870	1.6780	0.2050	0.0115	0.0290

Table 7 EDS analysis of Zr and Ti amount in the oxide-added cast Al 7075.

Alloy System	Wt.% Zr	Wt.% Ti
A	---	---
B	0.04 – 0.22	---
C	---	0.01 – 0.05
D	0.36 – 0.77	0.03 – 0.04

The optical micrographs of oxide-added cast Al 7075 are shown in [Fig. 6\(a\) to \(d\)](#).

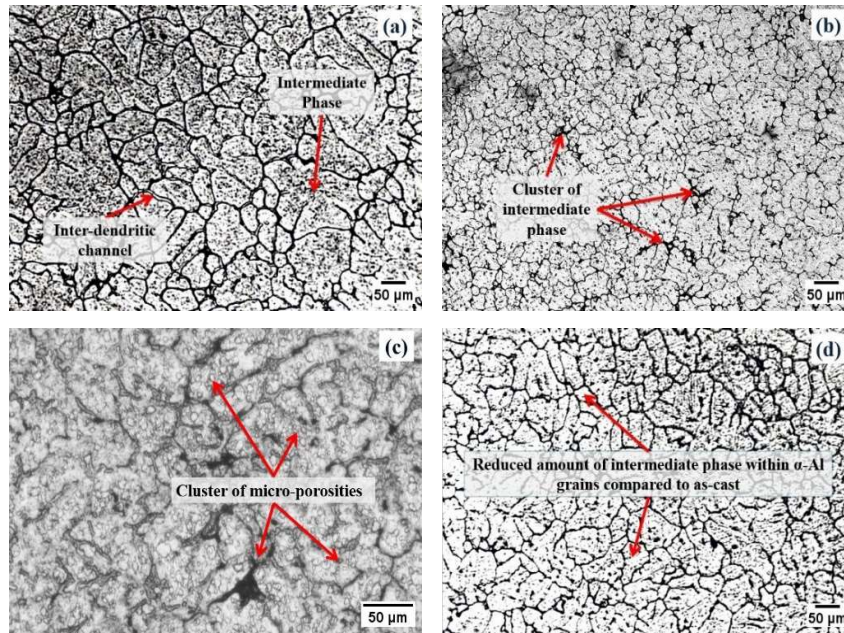


Fig. 6 Optical microstructure of Al7075; a) as-cast; and 2.5 wt.% added b) ZrO₂; c) TiO₂; d) ZrTiO₄.

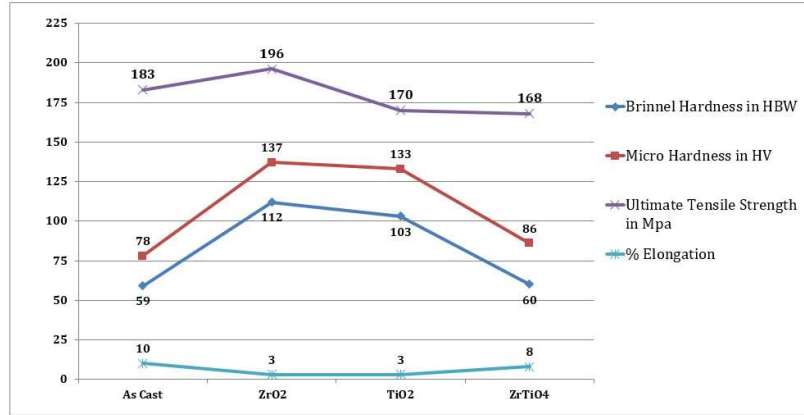


Fig. 7 Graphical presentation of mechanical properties of Al 7075; as-cast, and 2.5 wt.% added oxides.

The graphical presentation of mechanical properties is shown in Fig. 7. To confirm the presence of Ti and Zr after adding 2.5 wt. % of oxide, it is necessary to carry out SEM-EDS testing. The overall presence of Zr and Ti is significantly less. However, the localized presence can be confirmed by the SEM-EDS. The point EDS and area EDS were taken for all samples to study the intermediated phase distribution, as shown in Fig. 8(a) to (h).

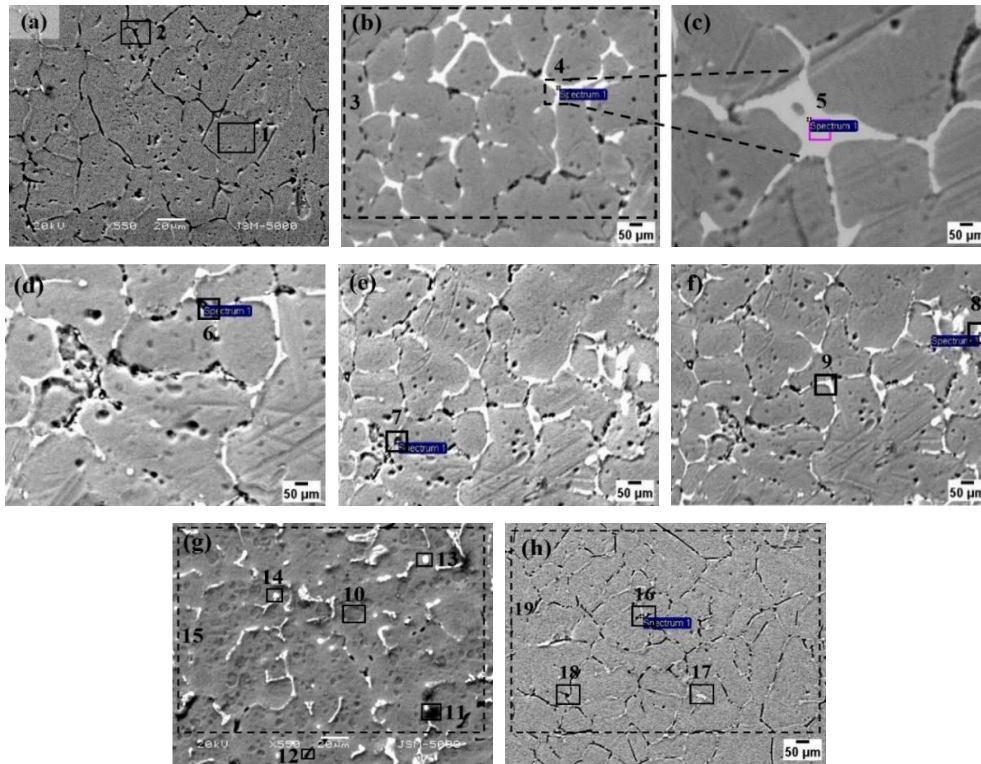


Fig. 8 SEM photographs of; (a) as-cast Al7075; (b to f) ZrO₂-added Al7075; (g) TiO₂-added Al7075; (h) ZrTiO₄ added Al7075.

Table 8 EDS analysis of selected point/area in Fig. 8 (in wt. %) and closest intermediate phases.

System	Points	Al	Zn	Mg	Cu	Zn/Mg	Closest Phase
As-cast	1	100.00	0.00	0.00	0.00	0.00	α (Al)
	2	99.65	0.11	0.24	0.00	0.46	T($\text{Al}_2\text{Mg}_3\text{Zn}_3$)
ZrO ₂ added	3 (Zr 0.05)	90.26	5.94	1.96	1.80	3.03	η (MgZn ₂)
	4 Zr (0.19)	50.53	23.07	11.18	15.04	2.06	T($\text{Al}_2\text{Mg}_3\text{Zn}_3$)
	5 (Zr 0.22)	45.84	24.77	12.66	16.55	1.96	T($\text{Al}_2\text{Mg}_3\text{Zn}_3$)
	6 (Zr 0.07)	69.42	12.44	3.07	13.88	4.06	η (MgZn ₂)
	7 (Zr 0.04)	79.11	7.75	2.74	2.51	2.83	η (MgZn ₂)
	8	87.14	4.85	2.36	1.42	2.06	η (MgZn ₂)
	9	41.88	17.27	10.37	13.4	1.67	T($\text{Al}_2\text{Mg}_3\text{Zn}_3$)
	10 (Ti 0.10)	91.38	3.88	1.05	0.45	3.70	η (MgZn ₂)
	11	42.29	2.84	2.04	0.56	1.39	T($\text{Al}_2\text{Mg}_3\text{Zn}_3$)
TiO ₂ added	12 (Ti 0.01)	65.59	5.97	9.70	1.84	0.62	T($\text{Al}_2\text{Mg}_3\text{Zn}_3$)
	13	66.60	12.03	3.51	8.21	3.43	η (MgZn ₂)
	14	55.77	2.01	0.90	2.39	2.23	η (MgZn ₂)
	15 (Ti 0.05)	84.90	4.99	1.56	1.28	3.20	η (MgZn ₂)
ZrTiO ₄ added	16 (Zr 0.36)	80.75	0.03	1.07	0.00	0.03	α (Al)
	17 (Ti 0.03)	81.46	0.00	0.39	0.00	0.00	α (Al)
	18 (Zr 0.77)	91.96	0.00	0.99	0.00	0.00	α (Al)
	19 (Ti 0.04)	95.87	0.00	0.47	0.00	0.00	α (Al)

Table 8 indicates the EDS analysis of all samples. In the last decade, many researchers reported intermediate phases of Al-Zn-Mg-Cu, such as MgZn₂, Al₂CuMg, Al₂Mg₃Zn₃, and Al₇Cu₂Fe. Zn, Mg, and Cu content determined the formation of these phases. Zn and Mg content significantly play a vital role in forming (η) MgZn₂ and (T) Al₂Mg₃Zn₃ phases based on Zn/Mg ratio. When Zn/Mg ratio > 2 forms the η phase, the T phase forms when Zn/Mg ratio < 2. Therefore, higher Mg content increases the probability of forming the T phase [107], [113].

6.2 Phase II: Effect of quenching medium on cast Al 7075.

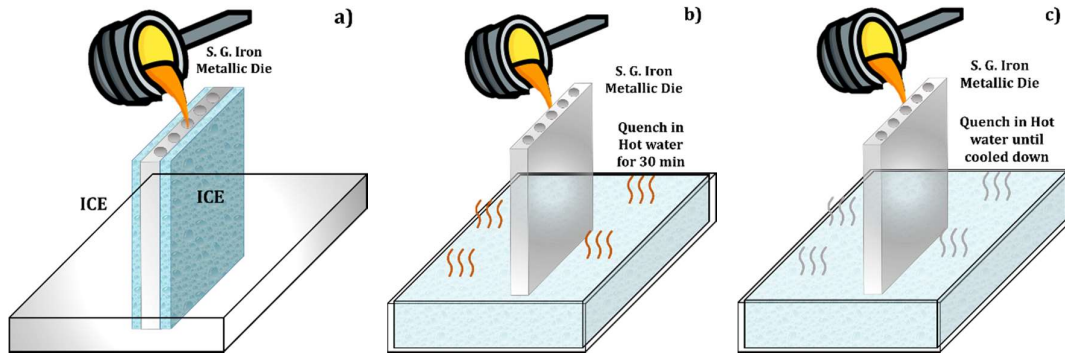


Fig. 9 Schematic diagram of quenching of cast Al 7075 during solidification in; a) ice, b) hot water for 30 min, and c) hot water until cooled down.

The different quenching conditions are used to cast Al 7075. Fig. 9 depicts three variants of casting: ice water, hot water for 30 minutes and hot water until it cooled down. In the case of hot water quenching, the die is wholly merged in the water by tilting horizontally after poring. The quenched and naturally aged for 2 years microstructure of cast Al 7075 is presented in Fig. 10(a-d), and Fig. 10(e-h), respectively. The microstructural morphology was changed depending on the thermal gradient at a solid-liquid interface. In the ice quenched, the microstructure is a mixture of equiaxed and columnar equiaxed grains, while in hot water quenched, dendrites and columnar dendrites are observed with the clustered solute segregation.

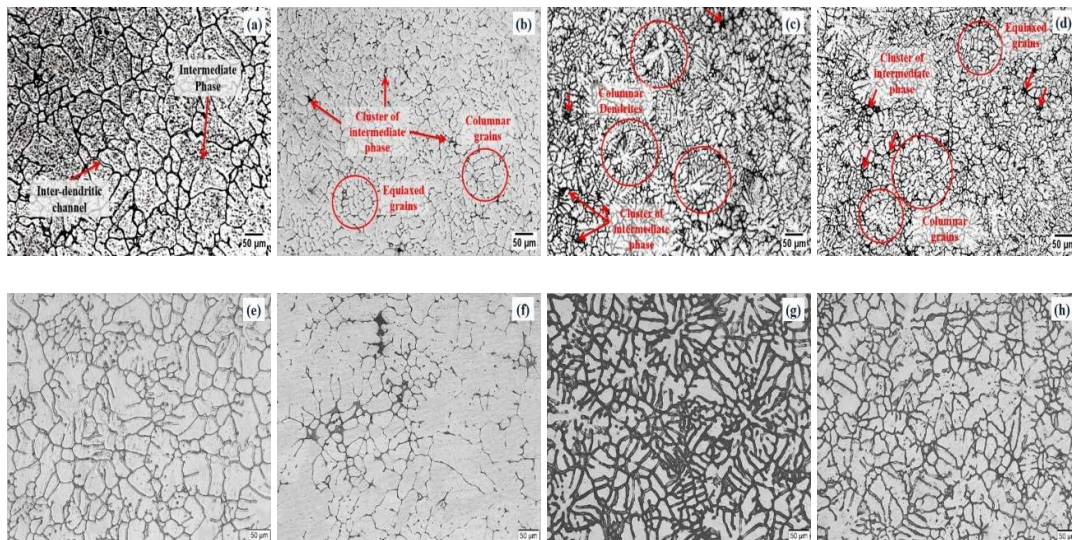


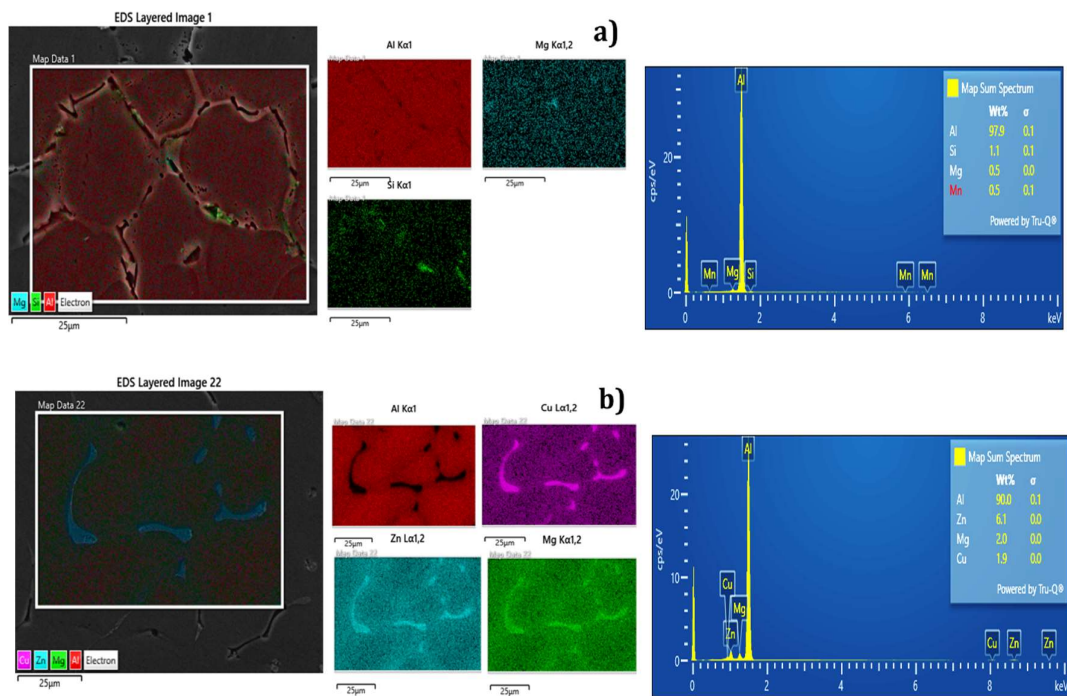
Fig. 10 Micrographs of cast Al 7075; a) as-cast, b) ice quench, c) hot water for 30 min, and d) hot water until cooled down; Micrographs of cast Al 7075 (naturally aged for 2 years) e) as-cast, f) ice quench, g) hot water for 30 min, and h) hot water until cooled down

The equiaxed dendrites are observed at some regions of hot water quenched micrographs. Solute segregation is observed at the grain boundary in naturally aged samples to form stable precipitates. The mechanical properties of quenched samples are presented in [Table 9](#).

Table 9 Mechanical properties of Al 7075; as-cast, quenched in ice, hot water for 30 min (H30), and hot water until cooled down (HTC).

Mech. Properties	Alloy System (Quenching Media)			
	As-cast	Ice	H30	HTC
Hardness (BHN)	59	94	100	123
Hardness (BHN) (Naturally Aged)	89 (↑50.84%)	150 (↑59.57%)	164 (↑64.00%)	142 (↑15.44%)
Microhardness (HV _{0.5})	78	99	95	129
Microhardness (HV _{0.5}) (Naturally Aged)	82 (↑5.12%)	153 (↑54.54%)	172 (↑81.05%)	146 (↑13.17%)
Tensile Strength (MPa)	183	190	197	188
Elongation (%)	10	2	1.5	2

The hardness values of all variants are compared, and it is found that the highest hardness is achieved in quenched in hot water until cooled down. The tensile strength values are more or less similar, and no significant difference is observed. The elemental mapped area EDS layered images are shown in [Fig. 11](#).



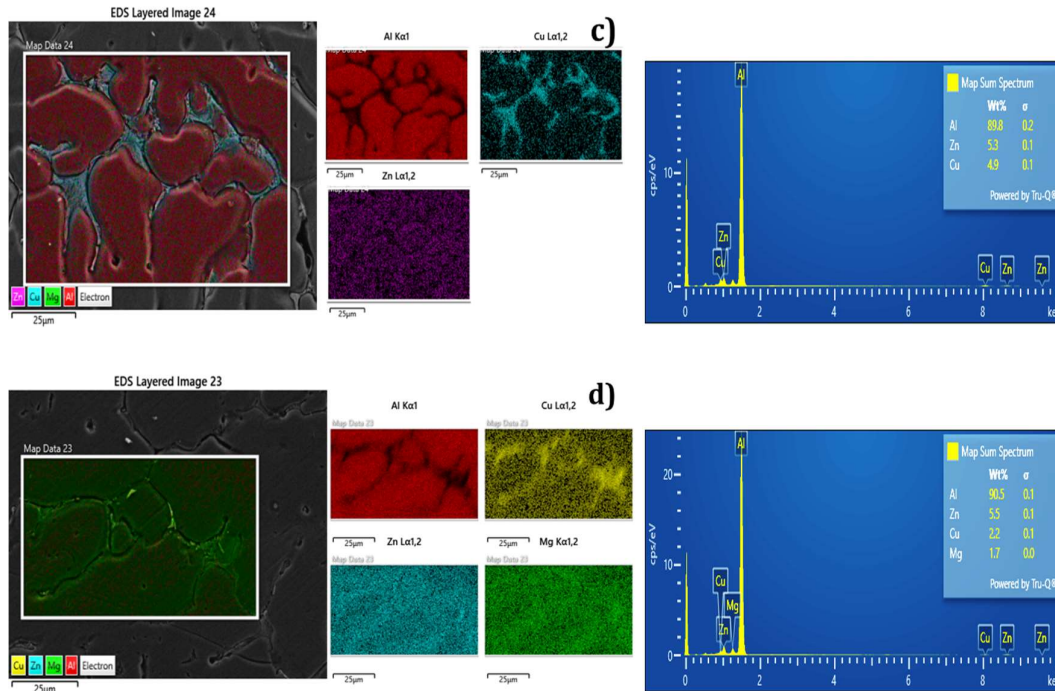


Fig. 11 Elemental mapped EDS layered images of Al 7075; a) as-cast, b) ice, c) H30, and d) HTC.

6.3 Phase III: Effect of double-step ageing on the oxide-added cast Al 7075

The methodology of producing oxide-added cast Al 7075 is similar to the one discussed in section 6.1. The as-cast and oxide-added cast Al 7075 are age hardened by double-step ageing treatment, as shown in Fig. 12. The microstructure, mechanical, and tribology properties of prepared samples are performed before and after heat treatment. SEM-EDS and XRD analysis confirms the presence of precipitates.

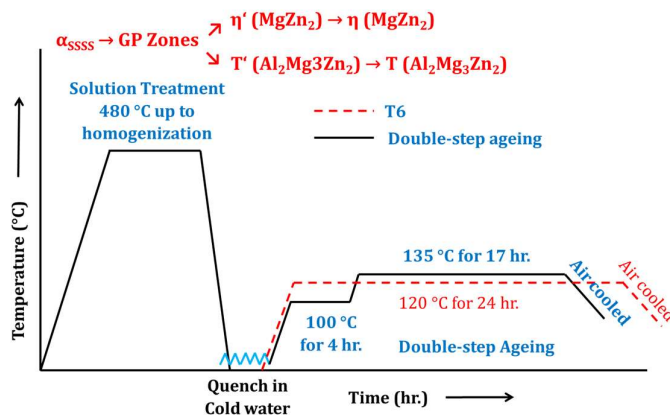


Fig. 12 Double-step ageing cycle for oxide-added cast Al 7075

The optical micrographs of all samples before and after heat treatment are shown in Fig. 13(a-h).

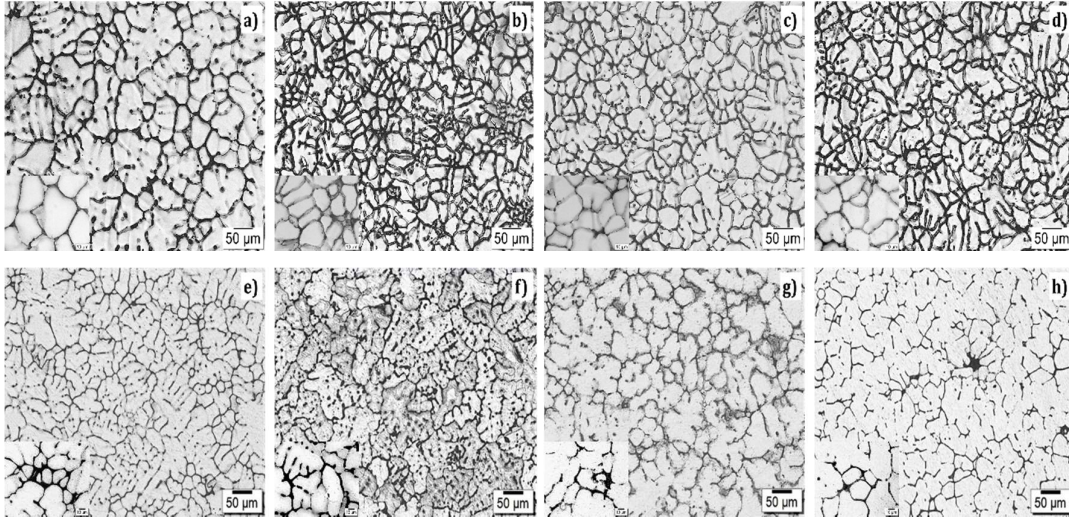


Fig. 13 Optical micrographs of oxide-added cast Al 7075 of as-cast, ZrO_2 -added, TiO_2 -added, and $ZrTiO_4$ -added before heat treatment (a-d) and after heat treatment (e-h), respectively.

The mechanical properties of oxide-added cast Al 7075 are presented in Table 10.

Table 10 Mechanical properties of as-cast, ZrO_2 -added, TiO_2 -added, and $ZrTiO_4$ -added cast Al 7075 before and after heat treatment.

Mech. Properties	Before HT				After HT			
	AS	Z	T	ZT	AS1	Z1	T1	ZT1
Hardness (BHN)	106	104	99	105	111 (↑4.71%)	160 (↑53.84%)	146 (↑47.47%)	140 (↑33.33%)
Microhardness ($HV_{0.5}$)	147	144	136	129	114 (↓22.44%)	171 (↑18.75%)	155 (↓13.97%)	111 (↓13.95%)
UTS (MPa)	147	212	189	184	279 (↑89.79%)	366 (↑72.64%)	317 (↑67.72%)	293 (↑59.23%)
Elong. (%)	2	2	2.5	3	2	1.5	1.5	1.5

The highest mechanical properties are achieved for ZrO_2 -added cast Al 7075 but at the cost of ductility. The tribology samples are carried out with a system parameter of 500, 700, and 1000 rpm for a fixed 1000 m distance with varying loads of 10, 20, 30, and 50N. Also, the wear loss in grams of ZrO_2 -added cast Al 7075 is significantly less for a 50N load at 1000 rpm.

6.4 Phase IV: Effect of different casting techniques on cast Al 7075

Different casting techniques like gravity die casting, green sand moulding, and investment casting is applied to produce the cast Al 7075. The described processes are differed by their mould characteristics and their final effect on the microstructure

and mechanical properties. The difference in the heat dissipation of the moulds creates an effective thermal gradient which causes a change in the microstructure and mechanical properties.

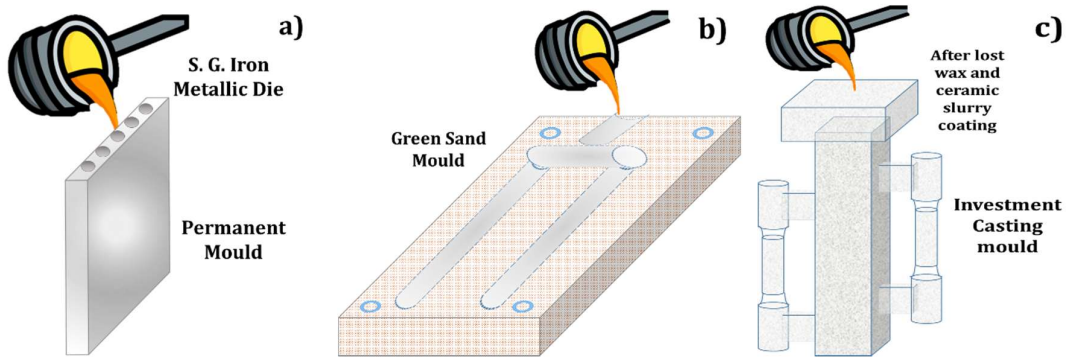


Fig. 14 Schematic illustration of casting techniques; a) gravity die casting, b) sand casting and c) investment casting.

The different casting techniques' micrographs are shown in Fig. 15(a-c) and after natural ageing in Fig. 15(d-f).

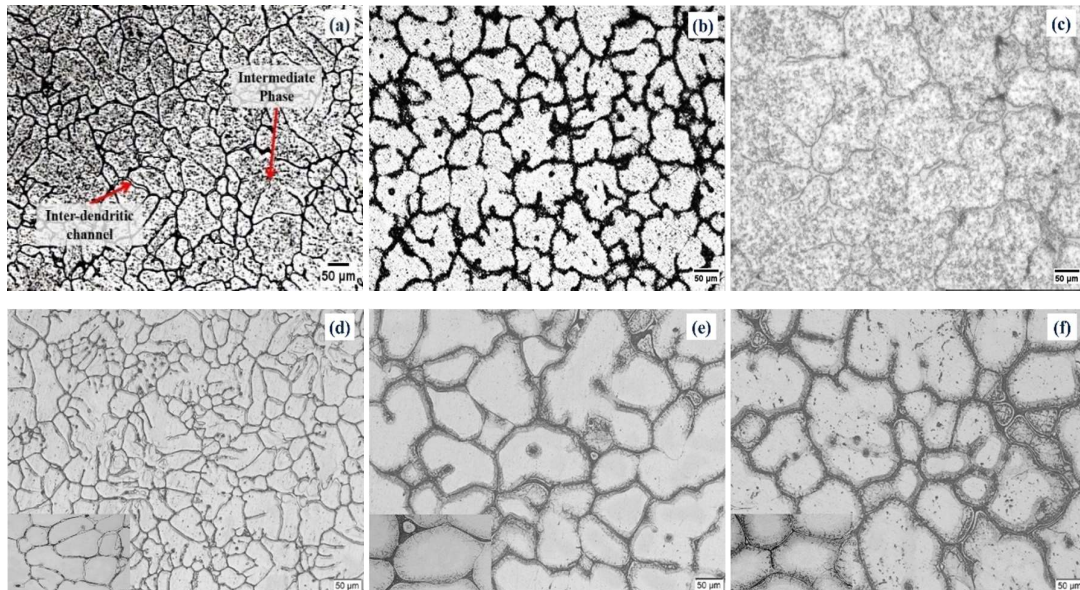


Fig. 15 Optical micrographs of different casting techniques of cast Al 7075; a) gravity die casting, b) sand casting, and c) investment casting; naturally aged (d-f), respectively.

From the microstructural study, the grain size of the cast Al 7075 for sand and investment castings is larger than die casting. Table 11 presents the mechanical properties of casting techniques. Hardness values are higher in sand and investment castings, but the tensile strength is not significantly increased due to coarser grains.

Table 11 Mechanical properties of cast Al 7075 by different casting techniques.

Mech. Properties	Casting techniques		
	As-cast	Sand Casting	Investment Casting
Hardness (BHN)	59	100	86
Hardness (BHN) (Naturally Aged)	89 (↑50.84%)	145 (↑45.00%)	140 (↑62.79%)
Microhardness (HV _{0.5})	78	105	90
Microhardness (HV _{0.5}) (Naturally Aged)	82 (↑5.12%)	161 (↑53.33%)	153 (↑70%)
Tensile Strength (MPa)	183	98	118
Elongation (%)	10	1.5	1.5

6.5 Phase V: Development of cast Al 7075 by alloy addition

Zinc is the primary alloying element of 7075 aluminium alloy. The addition of 5.1 – 6.1% zinc makes it heat treatable and high strength by precipitation hardening. Also, magnesium in the alloy ranges between 2.1 – 2.9% helps to produce the MgZn₂ phase. This principal strengthening precipitate is formed when the Zn to Mg ratio exceeds 2 weight percentages. Besides these two, Cu is added (1.2 – 2%) to improve the precipitation behaviour by forming the GP II zone and η' precipitate, which provides an early ageing stage. The chromium (0.18 – 0.28%) is added to inhibit the recrystallization, which controls the grain structure.

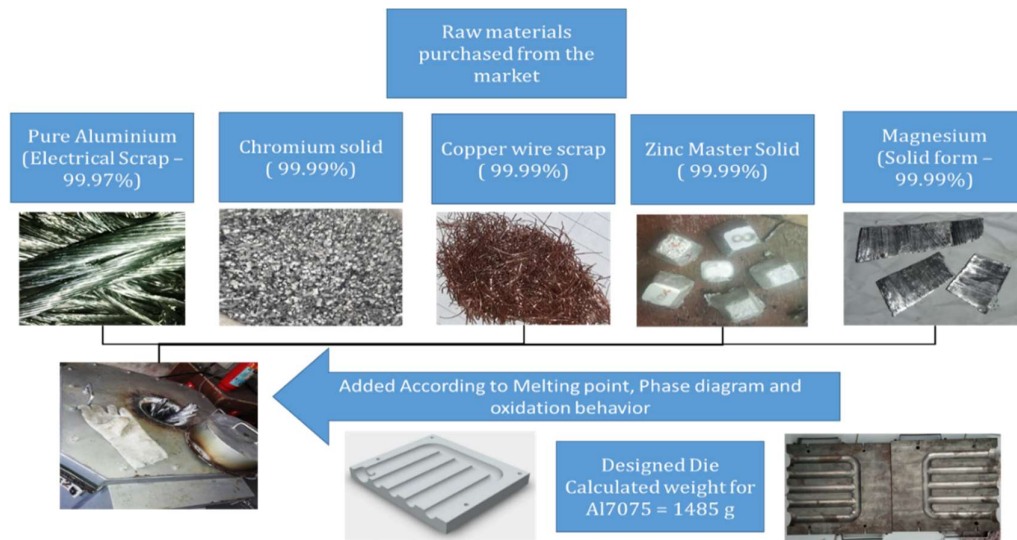


Fig. 16 Methodology of developed cast Al 7075.

The addition of alloying elements in pure aluminium has cost-effectively developed the 7075 aluminium alloy. Pure aluminium was in the form of electrical scrap, which is 99.97 % pure. The methodology of the developed cast Al 7075 is presented in Fig.

16. The micrographs and mechanical properties are shown in Fig. 17 and Table 12, respectively.

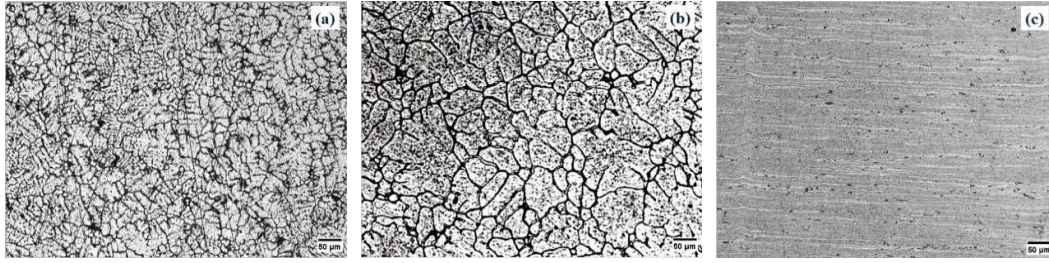


Fig. 17 Optical micrographs of Al 7075; a) developed cast 7075, b) cast 7075 from wrought, and c) wrought 7075.

Table 12 Comparative Mechanical properties of cast and wrought 7075 alloys.

Mech. Properties	Developed Al 7075		
	Developed 7075	Cast from Wrought	Wrought 7075
Hardness (BHN)	94	59	102
Microhardness (HV _{0.5})	146	78	112
Tensile Strength (MPa)	212	183	322
Elongation (%)	3%	10%	18%

7. Conclusions

The phase-wise conclusions are given as follows:

Phase I:

1. Oxide-added samples modified the microstructure by changing the distribution pattern of the non-equilibrium eutectic solid solution and finer the $\alpha(\text{Al})$ grains.
2. The presence of $\alpha(\text{Al})$ matrix coupled with dense and discontinuous eutectic with a cluster of micro-porosities at discrete location results in loss of mechanical properties in the case of 2.5 wt.% TiO_2 added Al7075.
3. SEM-EDS examination of ZrO_2 added Al7075 revealed the presence of 0.22 wt.% Zr, which hinders the recrystallization of the $\alpha(\text{Al})$ grains; additionally, dark spots confirm the presence of non-equilibrium eutectic phases, $\eta(\text{MgZn}_2)$, $\text{T}(\text{Al}_2\text{Mg}_3\text{Zn}_3)$, $\text{S}(\text{Al}_2\text{CuMg})$.
4. The distribution of the intermetallic phase influences the mechanical properties. ZrO_2 addition offers a 52% higher hardness value compared to as-cast Al7075. Tensile strength values remain all most same in all cases.

5. By considering Zn/Mg ratio, the EDS analysis confirms localized phases like (η) $MgZn_2$ and (T) $Al_2Mg_3Zn_3$.
6. Nuclei of Al_3Zr phase confirm by XRD analysis of ZrO_2 -added Al7075 alloy.
7. Comparatively, 2.5 wt. % TiO_2 -added Al7075 sample alters the mechanical properties by generating Al_1Ti_1 and Mg_1Zn_2 phases intermediate phase confirmed by XRD analysis.

Phase II:

1. Quenching media alter the solidification of the eutectic phase located at the grain boundary.
2. Due to the high thermal gradient, the independent nucleation results in an equiaxed grain structure observed in ice-quenched samples.
3. Hot water quenching for prolonged periods forms long and thin-columnar dendrites.
4. Hot water quenching for 30 min forms columnar and equiaxed dendrites and offers the highest tensile strength value of 197 MPa.
5. By changing the severity of quenching media, the hardness value varies from 59 BHN to 123 BHN in the case of as-cast and hot water quenching for a prolonged period.

Phase III:

1. The microstructure and mechanical properties of oxide-added cast Al 7075 are compared before and after double-step ageing. The excellent mechanical properties of ZrO_2 -added 7075 alloy are 212 MPa and 366 MPa before and after heat treatment.
2. Compared to other oxides addition, the average grain size of ZrO_2 -added 7075 alloy is 28.39 μm , which provides maximum grain boundary nucleating sites for precipitation.
3. Also, grain size significantly affects the dissolution time and concentration of Cu over the grain diameter for getting a homogeneous microstructure.
4. The microstructure of ZrO_2 -added 7075 alloy shows the uniform distribution of precipitates.
5. There is substantial improvement in the tensile strength and hardness values (BHN) after the heat treatment of all the samples, but the microhardness values increased by 18.75% for ZrO_2 while it decreased for other oxides.

Phase IV:

1. The grain structure of die-cast 7075 is columnar and equiaxed, while coarse globular grains are observed in the sand and investment cast 7075.
2. As-cast's eutectic phase segregation pattern is into the interdendritic channel, while grain boundary eutectic phase segregation, mainly at the triple junction, is observed in sand and investment cast 7075.
3. The tensile property of die-cast 7075 is 183 MPa, the highest of all, but the BHN hardness value is increased by 69.49% and 45.76 % of the sand cast and investment cast, respectively, compared to as-cast.

Phase V:

1. The successful development of Al 7075 is achieved after the 4th successive heat.
2. The early addition at high temperature is required to get chromium addition within a limit.
3. The magnesium is added lastly so that maximum recovery of magnesium is achieved.
4. The tensile strength and hardness of developed 7075 are 212 MPa which is higher than as-cast but lower than wrought.

Summarized Conclusion from all the Phases:

1. 2.5 wt. % ZrO₂ addition altered the eutectic segregation phase and converted α -Al grains into small equiaxed grains.
2. XRD analysis of ZrO₂-added cast 7075 alloy shows the presence of eutectic phases like η (MgZn₂), T(Al₂Mg₃Zn₃), and S(Al₂CuMg).
3. The highest mechanical properties are 196 MPa tensile strength and 112 BHN hardness observed in ZrO₂ addition.
4. Using localised chemical analysis by EDS and Zn/Mg ratios, (η) MgZn₂ and (T) Al₂Mg₃Zn₃ were confirmed.
5. The hot water quenching for 30 mins offers the highest tensile strength of 197 MPa and 100 BHN hardness value in the cast condition.
6. Double-step ageing treatment after ZrO₂ oxide addition offers 366 MPa tensile strength and 212 MPa before heat treatment.

7. By changing casting techniques, there is no significant to alter the eutectic phase segregation pattern, and finally, no substantial improvement in the mechanical properties.
8. Attempts were made to reduce the cost of 7075 alloy by alloy addition.

8. List of publications:

Sr. No.	Name of Author	Title of Paper	Journal /Conf. Proceeding	ISSN/I SBN No. Page Year	Publisher	Remarks/ Status
1.	Tej Parsania, Maulik Thakkar, Akshay More, Devang Mahant, Vandana Rao	Study on Modified heat treatment of Direct Chill Cast 7075 Aluminum Alloy	International Journal of Emerging Technology and Advanced Engineering (IJETAE)	ISSN: 2250-2459; Vol -5, Issue 11, Nov 2015		
2.	Devang Mahant, Vandana Rao	Mechanical Property and Microstructural Comparison of Wrought and Cast 7075 Aluminium Alloy	Proceedings of International Conference on Recent Advances in Metallurgy for Sustainable Development	ISBN: 978-93-88879-64-4 pp. 373-375 Year: 2018	New Delhi Publisher	Paper presented on 1-3 Feb 2018 and published
3.	Devang Mahant, Vandana Rao	Effect of addition of ZrO ₂ , TiO ₂ , and ZrTiO ₄ Oxides on Microstructure and Mechanical Properties of Cast 7075 Aluminum	Dogo Rangsang Research Journal	ISSN : 2347-7180; Vol-12 Issue-10 No. 02 October 2022	DRSR	Published
4.	Devang Mahant, Vandana Rao	Intermediate Phase Analysis of Cast Al7075 after the Addition of High-Temperature Oxides	International Conference on Advanced Technologies in Chemical, Construction, and Mechanical Sciences (iCATCHCOME 2023)	Materials Today Proceedings, Feb 2023	KPR Institute of Engg. and Tech. Coimbatore, Tamil Nadu.	Presented on 9 th Feb 2023 and accepted for publication in MATPAR in process.
5.	Devang Mahant, Vandana Rao	Investigation of microstructure and mechanical properties of ZrO ₂ ,	Indian Foundry Journal (IFJ)	ISSN: 0379-5446, Vol.69,	The Indian Institute of	Published in Feb 2023 issue.

		TiO ₂ , and ZrTiO ₄ added cast Al7075 alloy.		Issue II, Feb 2023	Foundry men	
6.	Devang Mahant, Rahul Yadav, Vandana Rao	Comparison of Wear Behaviour of Cast 7075 Aluminum by Oxide Additives	--	--	--	In the process of the journal publication

9. References

- [1] O. ALTUNTAŞ, “Enhancement of impact toughness properties of Al 7075 alloy via double aging heat treatment,” *Gazi Üniversitesi Fen Bilim. Derg. Part C Tasarım ve Teknol.*, vol. 10, no. 2, 2022, doi: 10.29109/gujsc.1108116.
- [2] H. M. Sabbar *et al.*, “AA7075-ZrO₂ Nanocomposites Produced by the Consecutive Solid-State Process: A Review of Characterisation and Potential Applications,” *Metals (Basel)*, vol. 11, no. 5, 2021, doi: 10.3390/met11050805.
- [3] P. X. Zhang, H. Yan, W. Liu, X. L. Zou, and B. B. Tang, “Effect of T6 heat treatment on microstructure and hardness of nanosized Al₂O₃ reinforced 7075 aluminum matrix composites,” *Metals (Basel)*, vol. 9, no. 1, 2019, doi: 10.3390/met9010044.
- [4] R. Karunanithi, K. S. Ghosh, and S. Bera, “Synthesis and characterization of TiO₂ dispersed Al 7075 micro- and nanocomposite,” *Adv. Mater. Res.*, vol. 984–985, pp. 313–318, 2014, doi: 10.4028/www.scientific.net/AMR.984-985.313.
- [5] G. S. Gan, Q. Gao, B. Yang, and S. De Gan, “Effect sedimentation of TiB₂ particles on the microstructure of 7075 Al alloy,” *Adv. Mater. Res.*, vol. 904, pp. 50–53, 2014, doi: 10.4028/www.scientific.net/AMR.904.50.
- [6] M. Zuo, M. Sokoluk, C. Cao, J. Yuan, S. Zheng, and X. Li, “Microstructure Control and Performance Evolution of Aluminum Alloy 7075 by Nano-Treating,” *Sci. Rep.*, vol. 9, no. 1, pp. 1–11, 2019, doi: 10.1038/s41598-019-47182-9.
- [7] X. Yang *et al.*, “Microstructural evaluation and mechanical properties of 7075 aluminum alloy prepared by controlled diffusion solidification,” *China Foundry*, vol. 16, no. 4, pp. 238–247, 2019, doi: 10.1007/s41230-019-9059-9.
- [8] F. Zhai, L. Wang, X. Gao, Y. Feng, S. Zhao, and L. Wang, “Phase evolution of a novel Al-Zn-Mg-Cu-Zr-Sm alloy during homogenization annealing treatment,” *Mater. Res. Express*, vol. 7, no. 7, 2020, doi: 10.1088/2053-1591/aba6bf.
- [9] V. J. Rao, Y. Das, and M. Sehgal, “Effect of Addition of MnO₂ and Mg in LM25 Alloy,” *Indian Foundry J.*, vol. 58, no. 10, pp. 3–6, 2012.
- [10] T. Parsania, M. Thakkar, A. More, D. Mahant, and V. Rao, “Study on Modified heat treatment of Direct Chill Cast 7075,” *Int. J. Emerg. Technol. Adv. Eng.*, vol. 5, no. 11, pp. 246–250, 2015, [Online]. Available: https://ijetae.com/files/Volume5Issue11/IJETAE_1115_43.pdf
- [11] Y. He, X. Zhang, and Z. Cao, “Effect of minor Cr, Mn, Zr, Ti and B on grain refinement of as-cast Al-Zn-Mg-Cu alloys,” *Xiyou Jinshu Cailiao Yu Gongcheng/Rare Met. Mater. Eng.*, vol. 39, no. 7, pp. 1135–1140, 2010, doi: 10.1016/s1875-5372(10)60108-7.
- [12] W. L. Zhang, D. H. Xiao, T. Li, J. Di Du, and D. Y. Ding, “Microstructure and mechanical properties of two-stage aged Al–Cu–Mg–Ag–Sm alloy,” *Rare Met.*, vol. 38, no. 1, pp. 42–51, 2019, doi: 10.1007/s12598-018-1137-4.
- [13] A. Ghosh, M. Ghosh, A. H. Seikh, and N. H. Alharthi, “Phase transformation and dispersoid evolution for Al-Zn-Mg-Cu alloy containing Sn during homogenisation,” *J. Mater. Res. Technol.*, vol. 9, no. 1, pp. 1–12, 2020, doi: 10.1016/j.jmrt.2019.08.055.
- [14] T. Li, S. C. Wang, and K. H. Zheng, “Effect of Al-5Ti-1B grain refiner on microstructure and mechanical properties of 7075 aluminum alloy,” *Mater. Sci. Forum*, vol. 817, pp. 331–336, 2015, doi: 10.4028/www.scientific.net/MSF.817.331.
- [15] M. Vlach *et al.*, “Influence of Heat Treatment on Microhardness and Phase Transformations in Cast and Homogenized 7075(-Sc-Zr) Aluminium Alloys,” *Diffus. Found.*, vol. 27, pp. 25–34, 2020, doi: 10.4028/www.scientific.net/df.27.25.
- [16] S. H. Wang *et al.*, “Microstructure of Al-Zn-Mg-Cu-Zr-0.5Er alloy under as-cast and homogenization conditions,” *Trans. Nonferrous Met. Soc. China (English Ed.)*, vol. 21, no. 7, pp. 1449–1454, 2011, doi: 10.1016/S1003-6326(11)60880-7.
- [17] W. Jie, “Solute redistribution and segregation in solidification processes,” *Sci. Technol. Adv. Mater.*, vol. 2, no. 1, pp. 29–35, 2001, doi: 10.1016/S1468-6996(01)00022-5.

- [18] K. Jiang, Y. Lan, Q. Pan, and Y. Deng, "Effect of the Zn/Mg Ratio on Microstructures, Mechanical Properties and Corrosion Performances of Al-Zn-Mg Alloys.," *Mater. (Basel, Switzerland)*, vol. 13, no. 15, Jul. 2020, doi: 10.3390/ma13153299.
- [19] O. N. Senkov, R. B. Bhat, S. V. Senkova, and J. D. Schloz, "Microstructure and properties of cast ingots of Al-Zn-Mg-Cu alloys modified with Sc and Zr," *Metall. Mater. Trans. A Phys. Metall. Mater. Sci.*, vol. 36, no. 8, pp. 2115–2126, 2005, doi: 10.1007/s11661-005-0332-8.
- [20] X. G. Fan, D. M. Jiang, Q. C. Meng, B. Y. Zhang, and T. Wang, "Evolution of eutectic structures in Al-Zn-Mg-Cu alloys during heat treatment," *Trans. Nonferrous Met. Soc. China (English Ed.)*, vol. 16, no. 3, pp. 577–581, 2006, doi: 10.1016/S1003-6326(06)60101-5.
- [21] B. Morere, R. Shahani, C. Maurice, and J. Driver, "The influence of Al₃Zr dispersoids on the recrystallization of hot-deformed AA 7010 alloys," *Metall. Mater. Trans. A Phys. Metall. Mater. Sci.*, vol. 32, no. 3, pp. 625–632, 2001, doi: 10.1007/s11661-001-0079-9.
- [22] J. R. Davis, "Aluminium and Aluminium Alloys," in *Alloying: Understanding the Basic*, J. R. Davis, Ed. ASM International, 2001, pp. 351–416. doi: <https://doi.org/10.31399/asm.tb.aub.t61170351>.
- [23] M. A. Khan *et al.*, "Enhanced tensile strength in an Al-Zn-Mg-Cu alloy via engineering the precipitates along the grain boundaries," *J. Mater. Res. Technol.*, vol. 22, pp. 696–705, 2023, doi: 10.1016/j.jmrt.2022.11.155.
- [24] R. Huang *et al.*, "Effects of Mg contents on microstructures and second phases of as-cast Al-Zn-Mg-Cu alloys," *J. Mater. Res. Technol.*, vol. 21, pp. 2105–2117, 2022, doi: 10.1016/j.jmrt.2022.10.050.
- [25] C. Liu, A. Davis, J. Fellowes, P. B. Prangnell, D. Raabe, and P. Shanthraj, "CALPHAD-informed phase-field model for two-sublattice phases based on chemical potentials: η -phase precipitation in Al-Zn-Mg-Cu alloys," *Acta Mater.*, vol. 226, p. 117602, 2022, doi: 10.1016/j.actamat.2021.117602.
- [26] WA Alloys, "International Alloy Designations and Chemical Composition Limits for Wrought Aluminum and Wrought Aluminum Alloys Use of the Information," *Alum. Assoc. Inc.*, no. August, 2018, [Online]. Available: www.aluminum.org
- [27] A. P. Mouritz, *Introduction to Aerospace Materials*. 2012. doi: 10.2514/4.869198.
- [28] T. Materials and I. Company, "Properties and Selection: Nonferrous Alloys and Special-Purpose Materials," *Prop. Sel. Nonferrous Alloy. Spec. Mater.*, 1990, doi: 10.31399/asm.hb.v02.9781627081627.
- [29] J. Jensin Joshua and A. Abraham Eben Andrews, "Design of experiments to optimize casting process of aluminum alloy 7075 in addition of TiO₂ using Taguchi method," *Mater. Today Proc.*, vol. 33, no. xxxx, pp. 3353–3358, 2020, doi: 10.1016/j.matpr.2020.05.164.
- [30] C. Kannan and R. Ramanujam, "Comparative study on the mechanical and microstructural characterisation of AA 7075 nano and hybrid nanocomposites produced by stir and squeeze casting," *J. Adv. Res.*, vol. 8, no. 4, pp. 309–319, 2017, doi: 10.1016/j.jare.2017.02.005.
- [31] A. Baradeswaran and A. Elaya Perumal, "Study on mechanical and wear properties of Al 7075/Al₂O₃/graphite hybrid composites," *Compos. Part B Eng.*, vol. 56, pp. 464–471, 2014, doi: 10.1016/j.compositesb.2013.08.013.
- [32] S. Suresh, G. H. Gowd, and M. L. S. Devakumar, "Mechanical and wear Characteristics of Aluminium Alloy 7075 Reinforced with Nano-Aluminium Oxide/ Magnesium Particles by Stir casting Method," *Mater. Today Proc.*, vol. 24, pp. 273–283, 2020, doi: 10.1016/j.matpr.2020.04.276.
- [33] Vijay Kumar Navuluri | Prasanna Nagasai Bellamkonda | Srikanth Sudabathula, "Characterization of Graphite and Zirconium Oxide on Al 7075 Metal Matrix Composites MMCS Fabricated by Stir Casting Technique," *Int. J. Trend Sci. Res. Dev.*, vol. 3, no. 5, pp. 820–823, 2019, doi: <https://doi.org/10.31142/ijtsrd26513>.
- [34] M. Ravikumar, H. N. Reddappa, R. Suresh, E. R. Babu, and C. R. Nagaraja, "Study on micro-nano sized al₂ o₃ particles on mechanical, wear and fracture behavior of al7075 metal matrix composites," *Frat. ed Integrita Strutt.*, vol. 15, no. 58, pp. 166–178, 2021, doi: 10.3221/IGF-ESIS.58.12.
- [35] Y. Sun, C. Zhang, B. Liu, Q. Meng, S. Ma, and W. Dai, "Reduced graphene oxide reinforced 7075 Al matrix composites: Powder synthesis and mechanical properties," *Metals (Basel)*, vol. 7, no. 11, 2017, doi: 10.3390/met7110499.

- [36] A. Raturi, K. K. S. Mer, and P. Kumar Pant, "Synthesis and characterization of mechanical, tribological and micro structural behaviour of Al 7075 matrix reinforced with nano Al₂O₃ particles," *Mater. Today Proc.*, vol. 4, no. 2, pp. 2645–2658, 2017, doi: 10.1016/j.matpr.2017.02.139.
- [37] A. kumar Gajakosh, R. Keshavamurthy, T. Jagadeesha, and R. S. Kumar, "Investigations on mechanical behavior of hot rolled Al7075/TiO₂/Gr hybrid composites," *Ceram. Int.*, vol. 47, no. 10, pp. 14775–14789, 2021, doi: 10.1016/j.ceramint.2020.10.236.
- [38] U. B. G. Krishna, B. Vasudeva, V. Auradi, and M. Nagaral, "Effect of Percentage Variation on Wear Behaviour of Tungsten Carbide and Cobalt Reinforced Al7075 Matrix Composites Synthesized by Melt Stirring Method," *J. Bio- Tribo-Corrosion*, vol. 7, no. 3, pp. 1–8, 2021, doi: 10.1007/s40735-021-00528-1.
- [39] M. Imran and A. R. A. Khan, "Characterization of Al-7075 metal matrix composites: A review," *J. Mater. Res. Technol.*, vol. 8, no. 3, pp. 3347–3356, 2019, doi: 10.1016/j.jmrt.2017.10.012.
- [40] R. R. Veeravalli, R. Nallu, and S. Mohammed Moulana Mohiuddin, "Mechanical and tribological properties of AA7075-TiC metal matrix composites under heat treated (T6) and cast conditions," *J. Mater. Res. Technol.*, vol. 5, no. 4, pp. 377–383, 2016, doi: 10.1016/j.jmrt.2016.03.011.
- [41] R. Manikandan, T. V. Arjunan, and A. R. Akhil, "Studies on micro structural characteristics, mechanical and tribological behaviours of boron carbide and cow dung ash reinforced aluminium (Al 7075) hybrid metal matrix composite," *Compos. Part B Eng.*, vol. 183, no. Al 7075, p. 107668, 2020, doi: 10.1016/j.compositesb.2019.107668.
- [42] T. P. Reddy, S. J. Kishore, P. C. Theja, and P. P. Rao, "Development and wear behavior investigation on aluminum-7075/B4C/fly ash metal matrix composites," *Adv. Compos. Hybrid Mater.*, vol. 3, no. 2, pp. 255–265, 2020, doi: 10.1007/s42114-020-00145-5.
- [43] A. Bhowmik, D. Dey, and A. Biswas, "Microstructure, mechanical and wear Behaviour of AL7075/SiC Aluminium matrix composite fabricated by stir casting," *Indian J. Eng. Mater. Sci.*, vol. 28, no. 1, pp. 46–54, 2021, doi: 10.56042/ijems.v28i1.35558.
- [44] R. Srinivasan, K. Hariharan, S. A. Jeyanthan, M. Kamalesh, and I. Ali, "Effect of addition of titanium carbide and graphite reinforcement on Al7075 hybrid metal matrix composites by gravity stir casting method," *Mater. Today Proc.*, vol. 62, pp. 86–93, 2022, doi: <https://doi.org/10.1016/j.matpr.2022.02.272>.
- [45] A. Rajasekaran and R. Pugazhenthii, "Study of mechanical properties of stir casted Al7075/SiCp composites after thermomechanical treatment," *Mater. Today Proc.*, vol. 22, no. xxxx, pp. 766–771, 2020, doi: 10.1016/j.matpr.2019.10.131.
- [46] A. Bhowmik, D. Chakraborty, D. Dey, and A. Biswas, "Investigation on wear behaviour of Al7075-SiC metal matrix composites prepared by stir casting," *Mater. Today Proc.*, vol. 26, no. xxxx, pp. 2992–2995, 2019, doi: 10.1016/j.matpr.2020.02.617.
- [47] S. Rajaram, T. Subbiah, P. K. Mahali, and M. Thangaraj, "Effect of Age-Hardening Temperature on Mechanical and Wear Behavior of Furnace-Cooled Al7075-Tungsten Carbide Composite," *Materials (Basel)*, vol. 15, no. 15, 2022, doi: 10.3390/ma15155344.
- [48] C. Kar and B. Surekha, "Characterisation of aluminium metal matrix composites reinforced with titanium carbide and red mud," *Mater. Res. Innov.*, vol. 25, no. 2, pp. 67–75, 2021, doi: 10.1080/14328917.2020.1735683.
- [49] B. Rajeswari, K. S. Amirthagadeswaran, and K. Ramya, "Microstructural studies of aluminium 7075-Silicon carbide- alumina metal matrix composite," *Adv. Mater. Res.*, vol. 984–985, pp. 194–199, 2014, doi: 10.4028/www.scientific.net/AMR.984-985.194.
- [50] V. Rao, N. Ramanaiah, and M. Sarcar, "Dry Sliding Wear Behavior of Al7075 Reinforced with Titanium Carbide (TiC) Particulate Composites Dry Sliding Wear Behavior of Al7075 Reinforced with Titanium Carbide (TiC) Particulate Composites Mechanical Engineering Department , Andhra University C," *Conference*, vol. proceeding, no. February 2016, pp. 2–7, 2015.
- [51] A. Prasad Reddy, P. Vamsi Krishna, R. Narasimha Rao, and N. V. Murthy, "Silicon Carbide Reinforced Aluminium Metal Matrix Nano Composites-A Review," *Mater. Today Proc.*, vol. 4, no. 2, pp. 3959–3971, 2017, doi: 10.1016/j.matpr.2017.02.296.
- [52] S. Devaganesh, P. K. D. Kumar, N. Venkatesh, and R. Balaji, "Study on the mechanical and

- tribological performances of hybrid SiC-Al7075 metal matrix composites,” *J. Mater. Res. Technol.*, vol. 9, no. 3, pp. 3759–3766, 2020, doi: 10.1016/j.jmrt.2020.02.002.
- [53] R. S. Harish, M. Sreenivasa Reddy, and J. Kumaraswamy, “Mechanical behaviour of Al7075 alloy Al₂O₃/E-Glass hybrid composites for automobile applications,” *Mater. Today Proc.*, vol. 72, pp. 2186–2192, 2023, doi: <https://doi.org/10.1016/j.matpr.2022.08.460>.
- [54] A. Baradeswaran and A. Elaya Perumal, “Influence of B₄C on the tribological and mechanical properties of Al 7075-B₄C composites,” *Compos. Part B Eng.*, vol. 54, no. 1, pp. 146–152, 2013, doi: 10.1016/j.compositesb.2013.05.012.
- [55] P. Maji, R. K. Nath, P. Paul, R. K. Bhogendro Meitei, and S. K. Ghosh, “Effect of processing speed on wear and corrosion behavior of novel MoS₂ and CeO₂ reinforced hybrid aluminum matrix composites fabricated by friction stir processing,” *J. Manuf. Process.*, vol. 69, no. June, pp. 1–11, 2021, doi: 10.1016/j.jmapro.2021.07.032.
- [56] G. Anbuechziyan, B. Mohan, N. Senthilkumar, and R. Pugazhenti, “Synthesis and Characterization of Silicon Nitride Reinforced Al–Mg–Zn Alloy Composites,” *Met. Mater. Int.*, vol. 27, no. 8, pp. 3058–3069, 2021, doi: 10.1007/s12540-020-00906-3.
- [57] S. Arun Kumar, J. Hari Vignesh, and S. Paul Joshua, “Investigating the effect of porosity on aluminium 7075 alloy reinforced with silicon nitride (Si₃N₄) metal matrix composites through STIR casting process,” *Mater. Today Proc.*, vol. 39, no. xxxx, pp. 414–419, 2020, doi: 10.1016/j.matpr.2020.07.690.
- [58] S. Rakshath, B. Suresha, R. Sasi Kumar, and I. Saravanan, “Dry sliding and abrasive wear behaviour of Al-7075 reinforced with alumina and boron nitride particulates,” *Mater. Today Proc.*, vol. 22, no. xxxx, pp. 619–626, 2020, doi: 10.1016/j.matpr.2019.09.010.
- [59] B. Kuldeep, K. P. Ravikumar, and S. Pradeep, “Effect of hexagonal boron nitrate on microstructure and mechanical behavior of Al7075 metal matrix composite producing by stir casting technique,” *Int. J. Eng. Trans. A Basics*, vol. 32, no. 7, pp. 1017–1022, 2019, doi: 10.5829/ije.2019.32.07a.15.
- [60] N. Ramadoss, K. Pazhanivel, and G. Anbuechziyan, “Synthesis of B₄C and BN reinforced Al7075 hybrid composites using stir casting method,” *J. Mater. Res. Technol.*, vol. 9, no. 3, pp. 6297–6304, 2020, doi: 10.1016/j.jmrt.2020.03.043.
- [61] V. Hotea, J. Juhasz, and F. Cadar, “Grain refinement of 7075Al alloy microstructures by inoculation with Al-Ti-B master alloy,” *IOP Conf. Ser. Mater. Sci. Eng.*, vol. 200, no. 1, 2017, doi: 10.1088/1757-899X/200/1/012029.
- [62] S. Sivasankaran, P. T. Harisagar, E. Saminathan, S. Siddharth, and P. Sasikumar, “Effect of nose radius and graphite addition on turning of AA 7075-ZrB₂ in-situ composites,” *Procedia Eng.*, vol. 97, pp. 582–589, 2014, doi: 10.1016/j.proeng.2014.12.286.
- [63] S. Suhael Ahmed and H. N. Girisha, “Experimental investigations on mechanical properties of Al7075/TiB₂/Gr hybrid composites,” *Mater. Today Proc.*, vol. 46, no. xxxx, pp. 6041–6044, 2020, doi: 10.1016/j.matpr.2021.01.960.
- [64] P. Loganathan, A. Gnanavelbabu, K. Rajkumar, and S. Ayyanar, “A comparative study of solid lubricant types on the microstructure and mechanical behaviour of AA7075-zirconium boride aerospace composites,” *IOP Conf. Ser. Mater. Sci. Eng.*, vol. 764, no. 1, 2020, doi: 10.1088/1757-899X/764/1/012001.
- [65] H. Kamali, E. Kamali, and M. Emany, “Effects of Zr additions on structure and tensile properties of an Al-4.5Cu-0.3Mg-0.05Ti (wt.%) alloy,” *China Foundry*, vol. 19, no. 1, pp. 9–16, 2022, doi: 10.1007/s41230-022-1094-2.
- [66] A. B. Kherdamand, S. Mirdamadi, Z. Lalegani, and B. Hamawandi, “Effect of Thermomechanical Treatment of Al-Zn-Mg-Cu with Minor Amount of Sc and Zr on the Mechanical Properties,” *Materials (Basel)*, vol. 15, no. 2, 2022, doi: 10.3390/ma15020589.
- [67] Q. Xing, X. Wu, J. Zang, L. Meng, and X. Zhang, “Effect of Er on Microstructure and Corrosion Behavior of Al–Zn–Mg–Cu–Sc–Zr Aluminum Alloys,” *Materials (Basel)*, vol. 15, no. 3, 2022, doi: 10.3390/ma15031040.
- [68] M. S. H. Al-Furjan, M. H. Hajmohammad, X. Shen, D. K. Rajak, and R. Kolahchi, “Evaluation of tensile strength and elastic modulus of 7075-T6 aluminum alloy by adding SiC reinforcing particles

- using vortex casting method,” *J. Alloys Compd.*, vol. 886, p. 161261, 2021, doi: 10.1016/j.jallcom.2021.161261.
- [69] Q. Tan *et al.*, “A novel strategy to additively manufacture 7075 aluminium alloy with selective laser melting,” *Mater. Sci. Eng. A*, vol. 821, no. June, 2021, doi: 10.1016/j.msea.2021.141638.
- [70] M. F. Kilicaslan, S. I. Elburni, and B. Akgul, “The Effects of Nb Addition on the Microstructure and Mechanical Properties of Melt Spun Al-7075 Alloy,” *Adv. Mater. Sci.*, vol. 21, no. 2, pp. 16–25, 2021, doi: 10.2478/adms-2021-0008.
- [71] N. G. Guruchannabasavaiah, V. Auradi, B. M. Nandeashaiah, S. B. Boppana, and B. N. Nishanth, “Investigation on the Microstructure and Mechanical Properties of Aluminum 7075 Reinforced with Different Weight Percentage of Tungsten Carbide and Cobalt Metal Matrix Hybrid Composites,” *IOP Conf. Ser. Mater. Sci. Eng.*, vol. 1013, no. 1, 2021, doi: 10.1088/1757-899X/1013/1/012021.
- [72] A. Bhowmik and A. Biswas, “Wear Resistivity of Al7075/6wt.%SiC Composite by Using Grey-Fuzzy Optimization Technique,” *Silicon*, vol. 14, no. 8, pp. 3843–3856, 2022, doi: 10.1007/s12633-021-01160-x.
- [73] N. U. Salmaan, S. A. Raja, and D. S. Robinson Smart, “Influence of silicon nitride, hafnium carbide and molybdenum disulfide to the wear behavior of al 7075 hybrid composites,” *Dig. J. Nanomater. Biostructures*, vol. 16, no. 3, pp. 959–967, 2021.
- [74] Y. F. Dong, B. H. Ren, K. Wang, J. Wang, and J. F. Leng, “Effects of graphene addition on the microstructure of 7075Al,” *Mater. Res. Express*, vol. 7, no. 2, 2020, doi: 10.1088/2053-1591/ab6faa.
- [75] A. Daoud, M. T. A. El-Khair, F. Fairouz, A. Lotfy, and E. Ahmed, “Microstructure aspects of 7075 Al-SiO₂ composite foams produced by direct melt foaming method,” *Key Eng. Mater.*, vol. 835 KEM, pp. 7–12, 2020, doi: 10.4028/www.scientific.net/KEM.835.7.
- [76] Q. Gao *et al.*, “Microstructure and Wear Resistance of TiB₂/7075 Composites Produced via Rheocasting,” *Metals (Basel)*, vol. 10, no. 8, p. 1068, 2020, doi: doi:10.3390/met10081068.
- [77] M. Nagaral, V. Auradi, S. A. Kori, and V. Shivaprasad, “Mechanical characterization and wear behavior of nano TiO₂ particulates reinforced Al7075 alloy composites,” *Mech. Adv. Compos. Struct.*, vol. 7, no. 1, pp. 71–78, 2020, doi: 10.22075/mac.2019.17075.1194.
- [78] J. Deng, J. Shen, H. Li, H. Chen, and F. Xie, “Investigation on microstructure, mechanical properties and corrosion behavior of Sc-contained Al-7075 alloys after solution-Aging treatment,” *Mater. Res. Express*, vol. 7, no. 9, 2020, doi: 10.1088/2053-1591/abb4fa.
- [79] Z. Lei, J. Bi, Y. Chen, X. Chen, Z. Tian, and X. Qin, “Effect of TiB₂ content on microstructural features and hardness of TiB₂/AA7075 composites manufactured by LMD,” *J. Manuf. Process.*, vol. 53, pp. 283–292, 2020, doi: 10.1016/j.jmapro.2020.02.036.
- [80] N. G. Yakoub, “Effect Of Nano-Zirconia Addition On The Tribological Behavior Of Al-7075 Nano Composites,” *Int. J. Sci. Technol. Res.*, vol. 9, no. 08, pp. 417–421, 2020.
- [81] I. Aziz and R. Bedien, “Effect of ZrO₂ Addition on Microstructure and Mechanical Properties of Al-Zn-Mg Alloy Matrix Composite,” *Eng. Technol. J.*, vol. 38, no. 12, pp. 1751–1757, 2020, doi: 10.30684/etj.v38i12a.336.
- [82] T. Gunasekaran, S. N. Vijayan, P. Prakash, and P. Satishkumar, “Mechanical properties and characterization of Al7075 aluminum alloy based ZrO₂ particle reinforced metal-matrix composites,” *Mater. Today Proc.*, no. December, 2020, doi: 10.1016/j.matpr.2020.11.114.
- [83] M. K. Sahu and R. K. Sahu, “Synthesis, microstructure and hardness of Al 7075/B₄C/Fly-ash composite using stir casting method,” *Mater. Today Proc.*, vol. 27, no. xxxx, pp. 2401–2406, 2019, doi: 10.1016/j.matpr.2019.09.150.
- [84] X. H. Chen and H. Yan, “Effect of nanoparticle Al₂O₃ addition on microstructure and mechanical properties of 7075 alloy,” *Int. J. Cast Met. Res.*, vol. 28, no. 6, pp. 337–344, 2015, doi: 10.1179/1743133615Y.0000000034.
- [85] W. Ruirui, Y. Zheng, and L. Qiushu, “Microstructure and mechanical properties of 7075 Al alloy based composites with Al₂O₃ nanoparticles,” *Int. J. Cast Met. Res.*, vol. 30, no. 6, pp. 337–340, 2017, doi: 10.1080/13640461.2017.1316954.
- [86] B. S. Sowrabh, B. M. Gurumurthy, Y. M. Shivaprakash, and S. S. Sharma, “Reinforcements,

- production techniques and property analysis of AA7075 matrix composites-a critical review,” *Manuf. Rev.*, vol. 8, 2021, doi: 10.1051/mfreview/2021029.
- [87] N. Sirajudeen, M. Abdur Rahman, S. Haque, R. Karunanithi, and S. Patnaik, “Influence of aging & varying weight fraction of Al₂O₃ particles on the mechanical behaviour & volumetric wear rate of Al 7075 alloy composite produced by liquid metallurgy route,” *Mater. Res. Express*, vol. 6, no. 8, 2019, doi: 10.1088/2053-1591/ab20b8.
- [88] S. Suresh, G. H. Gowd, and M. L. S. Deva Kumar, “Mechanical Properties of AA 7075/Al₂O₃/SiC Nano-metal Matrix Composites by Stir-Casting Method,” *J. Inst. Eng. Ser. D*, vol. 100, no. 1, pp. 43–53, 2019, doi: 10.1007/s40033-019-00178-1.
- [89] N. M. Rahma, K. M. Eweed, and A. A. Mohammed, “Investigation and improvement the Properties of 7075 AL/T6 Alloy using TiO₂ Nanomaterials,” *IOP Conf. Ser. Mater. Sci. Eng.*, vol. 454, no. 1, 2018, doi: 10.1088/1757-899X/454/1/012144.
- [90] P. B. Prakash, K. B. Raju, K. Venkatasubbaiah, and N. Manikandan, “Microstructure Analysis and Evaluation of Mechanical Properties of Al 7075 GNP’s Composites,” *Mater. Today Proc.*, vol. 5, no. 6, pp. 14281–14291, 2018, doi: 10.1016/j.matpr.2018.03.010.
- [91] P. Saritha, G. Saikumar, R. Venkatreddy, and P. R. Raju, “Mechanical Characterization and Wear Behaviour of Al7075 Alloy Reinforced With Alumina and Molybdenum Disulphide,” vol. 8, no. 6, pp. 395–404, 2018.
- [92] B. Subramaniam, B. Natarajan, B. Kaliyaperumal, and S. J. S. Chelladurai, “Investigation on mechanical properties of aluminium 7075 - boron carbide - coconut shell fly ash reinforced hybrid metal matrix composites,” *China Foundry*, vol. 15, no. 6, pp. 449–456, 2018, doi: 10.1007/s41230-018-8105-3.
- [93] S. K. Pasha, A. Sharma, and P. Tambe, “Mechanical properties and tribological behavior of Al7075 metal matrix composites: A review,” *Mater. Today Proc.*, vol. 56, pp. 1513–1521, 2022, doi: <https://doi.org/10.1016/j.matpr.2022.01.102>.
- [94] U. K. Mohanty and H. Sarangi, “Solidification of Metals and Alloys,” in *Casting Processes and Modelling of Metallic Materials*, Z. Abdallah and N. Aldoumani, Eds. Rijeka: IntechOpen, 2020. doi: 10.5772/intechopen.94393.
- [95] G. Li *et al.*, “Investigation of Solidification and Precipitation Behavior of Si-Modified 7075 Aluminum Alloy Fabricated by Laser-Based Powder Bed Fusion,” *Metall. Mater. Trans. A Phys. Metall. Mater. Sci.*, vol. 52, no. 1, pp. 194–210, 2021, doi: 10.1007/s11661-020-06073-9.
- [96] J. Sha *et al.*, “Si-Assisted Solidification Path and Microstructure Control of 7075 Aluminum Alloy with Improved Mechanical Properties by Selective Laser Melting,” *Acta Metall. Sin. (English Lett.)*, vol. 35, no. 9, pp. 1424–1438, 2022, doi: 10.1007/s40195-022-01419-1.
- [97] P. Vieth *et al.*, “Surface inoculation of aluminium powders for additive manufacturing of Al-7075 alloys,” *Procedia CIRP*, vol. 94, pp. 17–20, 2020, doi: 10.1016/j.procir.2020.09.004.
- [98] A. Ghosh, “Segregation in cast products,” *Sadhana*, vol. 26, no. April, pp. 5–24, 2001.
- [99] Nadella. R., D. G. Eskin., Du. Q., and Katgerman. L., “Macrosegregation in direct-chill casting of aluminium alloys,” *Prog. Mater. Sci.*, vol. 53, pp. 421–480, 2008, doi: 10.1016/j.pmatsci.2007.10.001.
- [100] X. Chen and H. Yan, “Solid-liquid interface dynamics during solidification of Al 7075-Al₂O₃np based metal matrix composites,” *Mater. Des.*, vol. 94, pp. 148–158, 2016, doi: <https://doi.org/10.1016/j.matdes.2016.01.042>.
- [101] F. Guili, Liu and Geliang, “Grain-boundary segregation and corrosion mechanism of Al-Zn-Mg-Cu ultra high strength aluminum alloys,” *Rare Met. Mater. Eng.*, vol. 38, pp. 1598–1601, 2009.
- [102] T. Wang *et al.*, “Materials & Design Extrusion of Unhomogenized Castings of 7075 Aluminum via SHAPE,” *Mater. Des.*, vol. 213, p. 110374, 2022, doi: 10.1016/j.matdes.2021.110374.
- [103] PRADYUMNA VISWAKARMA, S. SONI, and P. M. MISHRA, “An Effect of Reinforcement and Heat Treatment on AA7075 Metal Matrix Composite – A Review,” *Int. J. Mech. Prod. Eng. Res. Dev.*, vol. 8, no. 6, pp. 275–288, 2018, [Online]. Available: http://www.tjprc.org/view_full_paper.php?id=10694&type=html

- [104] W. Jiang, Z. Jiang, G. Li, Y. Wu, and Z. Fan, "Microstructure of Al / Al bimetallic composites by lost foam casting with Zn interlayer Microstructure of Al / Al bimetallic composites by lost foam casting with Zn," *Mater. Sci. Technol.*, vol. 0836, no. December, 2017, doi: 10.1080/02670836.2017.1407559.
- [105] Adrian P. Mouritz, *Introduction to aerospace materials*. Woodhead Publishing Limited, 2012.
- [106] Z. Chen, Y. Mo, and Z. Nie, "Effect of Zn Content on the Microstructure and Properties of Super-High Strength Al-Zn-Mg-Cu Alloys," *Metall. Mater. Trans. A*, vol. 44, no. 8, pp. 3910–3920, 2013, doi: 10.1007/s11661-013-1731-x.
- [107] L. I. Chunmei, C. Zhiqian, Z. Sumin, C. Nanpu, and C. Tianxiao, "Intermetallic phase formation and evolution during homogenization and solution in Al-Zn-Mg-Cu alloys," *Sci China Tech Sci*, vol. 56, no. 11, pp. 2827–2838, 2013, doi: 10.1007/s11431-013-5356-5.
- [108] W. X. Shu *et al.*, "Tailored Mg and Cu contents affecting the microstructures and mechanical properties of high-strength Al-Zn-Mg-Cu alloys," *Mater. Sci. Eng. A*, vol. 657, pp. 269–283, 2016, doi: 10.1016/j.msea.2016.01.039.
- [109] W. X. Shu *et al.*, "Solidification Paths and Phase Components at High Temperatures of High-Zn Al-Zn-Mg-Cu Alloys with Different Mg and Cu Contents," *Metall. Mater. Trans. A Phys. Metall. Mater. Sci.*, vol. 46, no. 11, pp. 5375–5392, 2015, doi: 10.1007/s11661-015-3050-x.
- [110] G. OZER and A. KARAASLAN, "Properties of AA7075 aluminum alloy in aging and retrogression and reaging process," *Trans. Nonferrous Met. Soc. China (English Ed.)*, vol. 27, no. 11, pp. 2357–2362, 2017, doi: 10.1016/S1003-6326(17)60261-9.
- [111] N. Zhang, C. Lei, H. Tang, and Q. Wang, "Double-step aging treatment of high strength Al-5 Mg-3Zn-1Cu(wt%) cast alloy," *Mater. Lett.*, vol. 322, p. 132514, 2022, doi: <https://doi.org/10.1016/j.matlet.2022.132514>.
- [112] N. M. Siddesh Kumar, Dhruthi, G. K. Pramod, P. Samrat, and M. Sadashiva, "A Critical Review on Heat Treatment of Aluminium Alloys," *Mater. Today Proc.*, vol. 58, pp. 71–79, 2022, doi: <https://doi.org/10.1016/j.matpr.2021.12.586>.
- [113] X. Li and J. J. Yu, "Modeling the effects of Cu variations on the precipitated phases and properties of Al-Zn-Mg-Cu alloys," *J. Mater. Eng. Perform.*, vol. 22, no. 10, pp. 2970–2981, 2013, doi: 10.1007/s11665-013-0588-x.